

FORECASTING MONTHLY RESIDENTIAL NATURAL GAS DEMAND IN TWO CITIES OF TURKEY USING JUST-IN-TIME-LEARNING MODELING

Burak Alakent¹ (burak.alakent@boun.edu.tr), Erkan Isikli² (isiklie@itu.edu.tr),
Cigdem Kadaifci² (kadaifci@itu.edu.tr), Tonguc S. Taspinar³ (tonguc.taspinar@socar.com.tr)

¹ Department of Chemical Engineering, Bogazici University, Bebek, 34342 Istanbul, Turkey.

² Department of Industrial Engineering, Faculty of Management, Istanbul Technical University, Macka,
Istanbul, 34367, Turkey.

³ SOCAR Türkiye, Vadistanbul Bulvar, Ayazağa Mahallesi, Azerbaycan Caddesi, No: 109-E, 1D Blok,
34485, Sarıyer, Istanbul, Turkey.

ABSTRACT

Natural gas (NG) is relatively a clean source of energy, particularly compared to fossil fuels, and worldwide consumption of NG has been increasing almost linearly in the last two decades. A similar trend can also be seen in Turkey, while another similarity is the high dependence on imports for the continuous NG supply. It is crucial to accurately forecast future NG demand (NGD) in Turkey, especially, for import contracts; in this respect, forecasts of monthly NGD for the following year are of utmost importance. In the current study, the historical monthly NG consumption data between 2014 and 2024 provided by SOCAR, the local residential NG distribution company for two cities in Turkey, Bursa and Kayseri, was used to determine out-of-sample monthly NGD forecasts for a period of one year and nine months using various time series models, including SARIMA and ETS models, and a novel proposed machine learning method. The proposed method, named Just-in-Time-Learning-Gaussian Process Regression (JITL-GPR), uses a novel feature representation for the past NG demand values; instead of using past demand values as column-wise separate features, they are placed on a two-dimensional (2-D) grid of year-month values. For each test point, a kernel function, tailored for the NGD predictions, is used in GPR to predict the query point. Since a model is constructed separately for each test point, the proposed method is, indeed, an example of JITL. The JITL-GPR method is easy to use and optimize, and offers a reduction in forecast errors compared to traditional time series methods and a state-of-the-art combination model; therefore, it is a promising tool for NGD forecasting in similar settings.

Keywords: Forecast Combination, Gaussian Process Regression, Online Learning, Time Series, SARIMA

INTRODUCTION

In the last few decades, there has been a shift in energy sources from fossil fuels to cleaner energy sources, such as wind and solar energy, mainly due to environmental concerns and related government regulations. However, these latter sources are dependent on weather conditions and require integration with grid technologies for continuous power generation. Natural gas (NG), typically, consists of (up to) ~95% of methane and 2-2.5% ethane-hexane+, with the remainder consisting of nitrogen, CO₂, oxygen and hydrogen, making NG closer to the cleaner side of the energy spectrum than fossil fuels. NG power plants are easy to build and highly reliable, making them invaluable for “clean” energy production. On the other hand, most countries depend on imports to maintain their NG supplies, and there is a delicate balance between imports and domestic demand. Storing excess imported gas above actual demand is difficult and would result in economic losses, while importing less than actual demand could result in a nationwide shortage. Therefore, accurate NGD predictions (NGDPs) are of utmost importance.

NGDP studies can be grouped by application area, which can vary from the whole world to cities, or by forecast horizon, which can be divided into (i) short-term, i.e., hourly to daily basis, (ii) medium-term, i.e., weekly to monthly basis, (iii) long-term, i.e., annual to decade basis, (iv) multi-term forecasting methods [1]. The focus in the literature has shifted from annual to daily forecasting methods from the 1970s to the present, possibly in line with advances in machine learning and forecasting methods; however, the share of medium-term studies in the entire NGDP literature has decreased from ~20% to ~15% during the same period [2], and the number of studies generating monthly forecasts is rather limited [3,4]. This may, in fact, be due to the dominant factors at different forecast horizons; monthly to quarterly forecasts are mostly and almost equally affected by temperature and economy [2], and both variables are difficult to predict for monthly periods [4,5].

A Brief Survey of NGDP Models

Here, we adopt the perspective proposed by a review study [2] for the analysis of the historical evolution of the NGPD literature. Early studies on short-time NGDP in the 1960s focused on using statistical models with weather-related variables as features, while recognizing the time-series nature, particularly the seasonality of the data, and suggesting the inclusion of lagged input and output variables in the models [6,7]. The influence of time series models, proposed by Box and Jenkins [8], on NGDP became particularly evident during the 1970s and 1980s. For

medium-term forecasting, a linear regression model consisting of heating degree days (HDD), cooling degree days (CDD), price of NG (PoG), number of customers (NoC), and NGD with a 12-month lag as inputs was used to obtain monthly NGDPs for residential customers in the US [9]. Monthly NGD for Taiwan was modeled using nonstationary seasonal autoregressive integrated moving average exogenous input (SARIMAX) models with lagged terms of temperature and PoG [10].

The priority given to nonlinear models increased by the late 1990s, possibly as a result of the advent of statistical learning methods [2]. Monthly NGDPs for Belgium were performed using an artificial neural network (ANN) model including exogenous features such as temperature, oil price and NoC [11]. The generation of one-to-three-day-ahead NG load forecasts was achieved by using a combination of ANN models, which incorporated the previous output, temperature, and wind speed as features. The integration of learners and the updating of learner weights during forecasting were shown to enhance prediction accuracy [12]. Similarly, combination of ANN models was shown to provide more accurate daily-to-weekly forecasts of NGD in Poland, compared to linear and quadratic regression models [13]. In another study, daily NGD loads for a one-month period were forecasted using two years of historical data in a Support Vector Regression (SVR) model, in which daily temperature forecasts during the test period were taken as simple averages of those of the previous two years during the same period [14]. In short-term NGD forecasting, Gil and Deferrari used a semi-empirical model to describe the relation of NGD with the number of users and temperature for short-term forecasts for Argentina [15].

In the last ~15 years, statistical models, time series methods and machine learning tools have been combined in coherent frameworks for accurate NGDPs. In short-term NGD forecasting, features related to weather, number of subscribers, and previous demand values have often been used to train learners, such as Linear Regression, Local SVR, Gradient Boosting (GB), and ANN models [16–18]. In recent studies, special attention has been given to the “data leakage” problem, especially related to weather-related variables; i.e., forecasts of exogenous variables are used in models for predicting future NGD values. For instance, one hour-to-60 hours ahead forecasts of temperature have been used in a model consisting of temperature-independent and temperature-dependent terms [19], and in a long short-term memory (LSTM) ANN model [20]. More recently, various deep learning architectures, such as the combination of convolutional NN (CNN) with attention modules to extract short-time relations, and LSTM models to capture longer-time relations, have been tailored for NGDP of various cities in China using training sets of moderate size, e.g., ~200-350 observations [21,22].

Among the few medium-term forecasting studies, mutual information on the exogenous variables, such as population, gross domestic product (GDP), PoG, and HDD, was used to select a subset of features to be incorporated into local linear neuro-fuzzy learner and Hodrick–Prescott filter to determine U.S. NGDPs for a 12-month period [23]. Extreme Learning Machine (ELM) and ANN models were shown to yield accurate monthly residential NGDPs for Karaj [24] and Tehran [25] in Iran, using weather-related variables as exogenous features; however, these studies used actual weather data during the test period, which makes the models difficult to use in practice.

NGDP Studies for Turkey

Demand for NG in Turkey is constantly increasing, and residential sector has accounted for >35% of its domestic NG consumption in 2023 [26]. While Turkey has been investing on NG resources, a large portion of Turkey’s source of NG is imports from Russia, Azerbaijan, Iran via the pipelines, and shipped Liquefied NG from Nigeria and Algeria [27]. NGDP for the entire country and individual cities in Turkey has been studied for the last ~25 years using various statistical and machine learning methods. One-day-ahead forecasts were conducted using SARIMAX and ANN models, and moving window linear regression model for Sakarya [28,29], multivariate adaptive regression splines (MARS), Lasso and Ridge Regression for Ankara [30–32], Fourier Series for Istanbul, Ankara and Eskisehir [33], SARIMAX, nonlinear ARX (NARX), ANN and LSTM models for Turkey [34], and ANN model for Istanbul [35]. The input features in these studies usually consisted of past demand values, instantaneous weather-related variables, the number of gas users, exchange rates and other economic variables.

In one of the earliest medium-term NGDP studies in Turkey, regression models, including HDD and previous prediction residuals as input features, were shown to improve monthly prediction accuracy compared to a single model for Eskisehir [36]. NGD in Istanbul was forecasted for a seven-month test period using ANN models, incorporating separately coded months, NoC and monthly average customers [37]. Relation of monthly NGD in Turkey and meteorological variables was examined using metaheuristic algorithms on additive regression models [38]. In a long-term NGDP analysis of Turkey spanning from 2005 to 2023, employing different base temperature scenarios, it was predicted that a 1°C change in the HDD base temperature would result in ~10% change in NG consumption [39]. In another study, daily NGDPs were modeled using HDD, exchange rate, and PoG as features in linear regression models. These models were developed for the purpose of annual forecasting, with the understanding that they may be applicable under stable and unstable economy scenarios [40].

Subset regression methods were used to select features among gross national product (GNP), population, and growth rate [41], while simulated annealing (SA) [42], hybrid SA+genetic algorithm (GA) [43], artificial bee colony algorithm [44], and cause-effect relationship-based Grey-prediction model [45] were used for forecasting Turkey's NGD under different scenarios. In contrast to scenario-based forecasts, long-term (>15 years) point predictions of annual NGD were obtained via a high-order ARI model [46], and modified logistic and linear equations, involving the (forecasted) population as the single predictor [47]. In a recent study, the fractional non-linear grey Bernoulli model, which was optimized by grey wolf optimization, was shown to yield better one-year ahead forecasting results compared to linear regression and ARIMA models using a limited data set of only 14 years [48]. A synopsis of NGDM studies conducted in Turkey is provided in the Appendix.

NGDP Studies Focusing on Medium-Term Forecasting Horizon

The extant studies have notable value for policy decisions and design purposes; however, most of them, particularly those pertaining to Turkey, use exogenous-variable models. In these models, either the actual (realized) values of the input features were used during the test period (ex-post forecasts), or the details of how input features were obtained during the test period were discussed superficially. One-day ahead estimations of variables related to weather might be helpful for short-term forecasting; however, forecasts of weather-related variables for longer than a week period would be less reliable, thereby decreasing the accuracy of exogenous variable models for monthly NGDP [15,49]. Scenario-based approaches, which use a palette of different forecast sets for future values of input features, have proven effective in long-term forecasting. However, the low-frequency change of exogenous variables, such as GDP, coupled with the challenging nature of accurately predicting variables like the inflation rate, poses a significant challenge in obtaining reliable monthly point NGDPs [50]. Consequently, methods employed for monthly forecasting (ex-ante forecasts) are rather limited in number and can be classified into two groups: (i) models that use the forecasted values of exogenous variables for future points and (ii) models that use previous NGD values, along with the possible inclusion of calendar information.

As an example of the former approach, Gil and Deferrari expanded their daily temperature predictions to monthly predictions by assuming a normal distribution of daily temperatures around a monthly mean, approximated by a simple periodic function within a year [15]. In a similar study, where one-day and one-month ahead residential NGD in Turkey were predicted using linear regression models with HDD, CDD, price and holiday effects as input features,

daily temperature was estimated using Ornstein-Uhlenbeck stochastic process models [51]. A nonlinear model including the predicted seasonal temperature effect was used to determine monthly NGDP in the Czech Republic [52].

The second approach entailed the integration of linear Hinges models to describe the seasonal behavior, augmented by a trend component, to determine monthly NGDP in Spain. The incorporation of explanatory variables proved instrumental in elucidating weekly effects [5]. ANN and adaptive neuro-fuzzy inference system (ANFIS) models using only previous NGD values without auxiliary features were shown to yield higher prediction accuracy compared to ARIMA model in forecasting NGD over a 15-week-period in Turkey [53]. In a study on forecasting monthly NG consumption for Istanbul, Turkey, over a one-year period, the authors used a set of features comprising the seasonal index, NG consumption at lag 12 (month), temperature, city population, and PoG [54]. NGDPs using an adjusted seasonal grey model over a four-year period [55], and Holt-Winters exponential smoothing and SARIMAX models for monthly periods [56], both yielded acceptable forecast accuracy for Turkey. Nonlinear grey Bernoulli model based on Hodrick-Prescott (HP) filter was shown to yield the smallest prediction error among other seasonal models in predicting monthly NGD values of European Union countries [4]. A comparison of ARIMA, NARNN, SVR, and LSTM models using the weekly NGD in Turkey during Covid pandemic, was conducted in a recent study for one-week ahead forecasts [57]. A study that combined CNN and LSTM models for forecasting daily NGDPs in Chinese cities used only previous NGD values for model training, demonstrating that deep learning architectures can also be used for medium-term NGDPs under a similar setting [21]. Quarterly NG consumption data in China was analyzed using moving average and seasonal indices to yield NG consumption forecasts until 2035 [58]. A recent study on an ensemble of ETS and SARIMA models, obtained via resampling the remainder of Seasonal-Trend decomposition using LOESS (STL) on NGD for 18 European countries, yielded a good prediction accuracy for a 12-month ahead period [3]. The Salp swarm algorithm, in conjunction with Extreme Gradient Boosting (XGB), was employed to forecast five-month ahead NGDPs for the UK and the Netherlands within a moving window (MW) frame [59].

Perspective of the Present Study

The monthly NGD data of Bursa and Kayseri, two cities in Turkey, from 2014 to 2024 were provided by The State Oil Company of Azerbaijan Republic (SOCAR), an Azerbaijani local NG distribution company employed in Turkey. SOCAR was established in 1992 with the mission of managing the nation's oil and natural gas industry. This globally recognized energy

giant plays a pivotal role in delivering the abundant energy resources of the Caspian Sea to global markets. SOCAR's activities span a broad range, including: (i) the exploration and operation of Azerbaijan's oil and natural gas reserves through the use of advanced technologies. As of 2023, SOCAR's production from reserves in the Caspian Sea amounted to approximately 34 million tons of oil and 35 billion cubic meters of natural gas annually. SOCAR's role in the refining of oil and the production of energy products is also noteworthy. The company's *Başkal* and *Yeni Heydar Aliyev* refineries possess a combined processing capacity of 7 million tons of crude oil per year. Furthermore, SOCAR has strategically invested in transportation infrastructure to facilitate the delivery of energy products to domestic and international markets, establishing a robust logistics network comprising pipelines and terminals. Approximately 50 million tons of oil are transported annually via the *Baku-Tbilisi-Ceyhan Pipeline*. Additionally, SOCAR Turkey Research, Development and Innovation Inc. (SOCAR Turkey R&D), established in 2019, develops innovative, sustainable, environmentally friendly, and market-oriented products and digital technologies, and provides R&D services to all its stakeholders with its deep-rooted experience in the energy sector. SOCAR has invested in various projects in Turkey, Georgia, and other countries to be among the global players in the energy sector. Notably, SOCAR has augmented its regional effectiveness through substantial investments, amounting to a total of 18.5 billion dollars. These investments have been made through initiatives such as the acquisition of PETKİM in Turkey and its subsequent integration with the recently established STAR Refinery, the completion of the Trans Anatolian Natural Gas Pipeline (TANAP) Project, and the acquisition and operation of natural gas distribution companies such as Bursagaz and Kayserigaz.

To comply with the specifications of the import agreements, it is necessary to make monthly NGD forecasts for the upcoming year. In the present study, a novel ex-ante NGDP method, namely Just-In-Time-Learning-Gaussian Process Regression (JITL-GPR), is proposed. The JITL-GPR model uses only the previous NGD values and calendar data, offering a more nuanced interpretation from an online learning perspective as opposed to batch learning. In batch learning, a constant model (or an ensemble of models) is constructed from a given (historical) dataset, and the response variable value of a new query point is predicted using this model. Conversely, in online learning, a model is continuously adapted or changed upon varying operating conditions [60–62]. The accuracy of a constant model relating inputs to outputs, derived using batch learning, is likely to degrade over time; therefore, relaxing the constant model assumption is an advantage of online learning [63]. Indeed, online learning methods have already been successfully used (rather implicitly) for NGDP: Linear learning

methods were found to demonstrate enhanced efficacy when used simultaneously with recursive [16], MW [1,19,59], or nearest neighbor (NN) [17] methods. Furthermore, the prediction accuracy of nonlinear learning methods was shown to increase when trained in an adaptive manner [12].

The novelties of JITL-GPR are as follows: (i) Instead of extracting trend-seasonality information directly and globally from the entire data, as most of the time series methods do, this information is captured indirectly through the selection of a convenient “window” of observations on a two-dimensional grid of the historical year-month plane. (ii) A convenient kernel is designed to exploit the trend-seasonality information to be used in GPR. (iii) The procedure is repeated for each query point, akin to Just-In-Time-Learning (JITL) or local learning [64], while recent information is also included, similar to a MW method [65,66]. Hence, the method yields predictions consistent with previous years, while adapting to changes in recent months. In comparison to conventional time series methodologies such as SARIMA and ETS, JITL-GPR was shown to exhibit superior accuracy in terms of NGDP estimation. Section 2 encompasses a concise overview of Time Series Methods, GPR and JITL. Following the presentation of the data’s specifics, a comprehensive discourse on the results obtained using time series methods and JITL-GPR is provided in Section 4. The final section proposes several future research directions.

THEORETICAL BACKGROUND

Time Series Modeling

Seasonal and Trend Decomposition using LOESS (STL)

The pattern of a time series can be decomposed into sub-patterns in many cases, thereby defining the various components of the series individually. This type of decomposition frequently enhances the accuracy of forecasting by facilitating a more profound comprehension of the series' behavior [67]. Consequently, decomposition of a time series is a useful instrument for the analysis of a series and the subsequent selection of a method for its modeling. In the present study, we employed the STL (seasonal-trend decomposition) procedure that consists of an inner loop nested inside an outer loop. Developed by [68], this non-parametric additive decomposition method provides a simple design based on local regression smoothing (LOESS) that is flexible in specifying the amounts of variation in the trend and seasonal components. It is widely regarded as a valuable tool for elucidating the underlying patterns in datasets that exhibit substantial seasonal effects. A notable strength of STL lies in its capacity to handle series with missing values, yielding robust trend and seasonal components that are not distorted by transient, aberrant behavior in the data [68]. In other words, it can accommodate non-fixed seasonal patterns and handle non-linear trends in the presence of outliers. The general form of the STL model can be expressed as follows in Equation 1:

$$y_t = (\alpha + \beta t) + S_t + \varepsilon_t = \hat{y}_t + \varepsilon_t \quad (1)$$

where y_t is the actual value of the time series at time point t ; $\alpha + \beta t$ corresponds to the trend component; S_t is the seasonal index at time point t ; ε_t is the error component at time point t . While STL can manage any kind of seasonality (i.e., weekly, monthly, or quarterly), allowing users to determine the trend's smoothness and enable the seasonal component to alter over time, it only offers additive decomposition capabilities and does not automatically handle calendar or trading day variations [69]. It can be implemented easily since it relies on numerical methods rather than mathematical modeling [70].

Seasonal Autoregressive Integrated Moving Average (SARIMA)

Along with smoothing methods, ARIMA is one of the most widely used and effective time series modeling approaches. It aims to describe the behavior of a time series based on autocorrelations [71]. This type of models posits that future values of a time series are generated

from a linear function of its past observations and some white noise errors. The model is specified by three parameters: p , the order of the autoregressive component; d , the order of the differencing required for the series to be mean stationary; and q , the order of the moving average component. Equation 2 illustrates an ARIMA(p, d, q) model:

$$\Delta^d y_t = \mu + \phi_1 \Delta^d y_{t-1} + \phi_2 \Delta^d y_{t-2} + \dots + \phi_p \Delta^d y_{t-p} - \theta_1 \varepsilon_{t-1} - \theta_2 \varepsilon_{t-2} - \dots - \theta_q \varepsilon_{t-q} \quad (2)$$

where $\Delta^d y_t$ is the d -th difference of the original series, ϕ_i is the parameter for the i^{th} autoregressive term, θ_j is the parameter for the j^{th} moving average term, and $i = \overline{1, p}$ and $j = \overline{1, q}$. For a comprehensive exposition on the underpinnings of ARIMA-type models, readers are directed to the seminal contributions of [72]. The ARIMA methodology was extended to incorporate seasonal trends along with primary stochastic trend to facilitate the modeling of time series characterized by periodicity and regular patterns across diverse time scales. Known as SARIMA, this type of model is denoted by ARIMA(p, d, q)(P, D, Q) $_s$, where D denotes the degree of seasonal differencing, P denotes the number of seasonal autoregressive components, Q denotes the number of seasonal moving average components, and s denotes the seasonal cycle (e.g., for monthly data with yearly seasonality, $s = 12$). Expressing a SARIMA model explicitly is tedious; therefore, lag polynomials are most often used. A scrambled mathematical representation of an ARIMA(0,1,1)(0,1,1) $_{12}$ model is formulated in Equation 3 below as an example:

$$\Delta_{12}^D \Delta^d y_t = \mu + \Theta_1 \theta_1 \varepsilon_{t-13} - \Theta_1 \varepsilon_{t-12} - \theta_1 \varepsilon_{t-1} + \varepsilon_t \quad (3)$$

where $\Delta_{12}^D y_t$ is the D -th seasonal difference of the original series and Θ_1 is the parameter for the seasonal moving average component.

Exponential Smoothing State Space Models (ETS)

State space models, first introduced in the late 1970s, offer a high degree of flexibility in the specification of parameters for level, trend, and seasonal components. This is primarily achieved through the use of two equations: the observation equation and the state equation [73]. As intrinsically non-parametric models, they are reliable and computationally efficient. For a more in-depth exploration of this topic, readers are directed to [74]. A notable distinction of state space models for exponential smoothing is the inclusion of an error component, in addition to the trend and seasonal components, which distinguishes them from the smoothing methods previously introduced in the related literature. This class of models is commonly denoted by

the acronym ETS(x, y, z), where x designates whether errors are additive (A) or multiplicative (M), y indicates the trend is additive or multiplicative nature, and z denotes the seasonality is additive or multiplicative character. To illustrate, the following two representations of the ETS(M,A,N) model are provided below. The general representation is given in Equations 4-6, whereas the state space representation is given in Equations 7-8. This is somewhat equivalent to Holt's linear method, but the errors in this case are multiplicative rather than additive.

$$\text{Forecast:} \quad \hat{y}_t = (L_{t-1} + B_{t-1})(1 + \varepsilon_t) \quad (4)$$

$$\text{Level:} \quad L_t = (1 + \alpha\varepsilon_t)(L_{t-1} + B_{t-1}) \quad (5)$$

$$\text{Trend:} \quad B_t = \alpha\beta(L_{t-1} + B_{t-1})\varepsilon_t + B_{t-1} \quad (6)$$

$$\text{Obs. Equation:} \quad y_t = \begin{bmatrix} 1 \\ 1 \end{bmatrix}^T \mathbf{x}_{t-1}(1 + \varepsilon_t) \quad (7)$$

$$\text{State Equation:} \quad \mathbf{x}_t = \begin{bmatrix} 1 & 1 \\ 0 & 1 \end{bmatrix} \mathbf{x}_{t-1} + \begin{bmatrix} 1 \\ 1 \end{bmatrix}^T \mathbf{x}_{t-1} \begin{bmatrix} \alpha \\ \beta \end{bmatrix} \varepsilon_t \quad (8)$$

where $\hat{y}_t = E[y_t | y_{t-1}, y_{t-2}, \dots, y_1]$ is the one-step-ahead forecast, L_t denotes the baseline value of the series at time point t , $\mathbf{x}_t = \begin{bmatrix} L_t \\ B_t \end{bmatrix}$ is the state vector and the one-step ahead forecast errors (estimation data), $\varepsilon_t = \frac{y_t - (L_{t-1} + B_{t-1})}{L_{t-1} + B_{t-1}}$, follow a normal distribution with zero mean and constant variance. The selection of the ETS model is contingent upon the characteristics of the time series, and estimation of model parameters is frequently executed through the Maximum Likelihood Estimation (MLE) technique. This approach involves maximizing the "likelihood" and thereby minimizing the sum of squared errors while optimizing the parameters. Table 1 presents a selection of the most commonly used ETS methods, along with their respective notations and references. A comprehensive overview of the equations in state space for every model in the ETS framework can be found in [69].

Table 1. Commonly used ETS models

Method	ETS Notation	Reference
Simple Exponential Smoothing (SES)	ETS(A,N,N)	[75]
Holt's Linear Trend method	ETS(A,A,N)	[76]
Holt-Winters' Additive Method	ETS(A,A,A)	[77]
Holt-Winters' Multiplicative Method	ETS(M,A,M)	[77]
Holt-Winters' Damped Method	ETS(A,A _d ,A)	[78]

Trigonometric Box-Cox transform, ARMA errors, Trend, and Seasonal Components (TBATS):

Integrating the principles of ETS and other methodologies, TBATS handle multi-frequent seasonality and non-linear trends. TBATS was introduced by [79] as an extension of ETS to model multiple seasonal patterns in a time series simultaneously. In the abbreviation TBATS, the first letter of each word indicates a particular aspect of the model: B = Box-Cox transformation, A = ARMA errors, T = Trend, and S = Seasonality. The first T indicates that a trigonometric formulation was adopted to model seasonality. The method employs a Box-Cox transformation to stabilize variance and incorporates ARMA components to enhance the accuracy of error modeling. For a detailed exposition of TBATS, readers are directed to consult [80].

The Aggregated Forecast Through Exponential Reweighting (AFTER):

This simple and efficient method was initially proposed by [81] as a means of combining heterogeneous forecast models. Subsequent modifications have been made [82], and the method has been applied to various cases [83] since its initial introduction. Considering individual model performance history and focusing on minimizing prediction error over time, AFTER adjusts the combination weights, which undergo an exponential decay that is based on the performance of the models. This approach stands in contrast to classical forecast combination methods, which are limited to fixed or predetermined weights. For a more detailed description of AFTER, the reader is referred to [84] and [85].

Gaussian Process Regression (GPR)

Bayesian linear regression (BLR) is a parametric model, consisting of basis functions evaluated at finite training points. Given a set of N data points $\{(\mathbf{x}_1, y_1), (\mathbf{x}_2, y_2) \dots (\mathbf{x}_N, y_N)\}$ with $\mathbf{x}_n \in \mathbb{R}^p$ and $y_n \in \mathbb{R}$, the response variable y_n is assumed to be normally distributed about the regression function, which is determined by the product of a basis function $\phi(\cdot)$ evaluated at \mathbf{x}_n and a parameter vector $\mathbf{w} \in \mathbb{R}^p$. This model is augmented with a Gaussian prior, specified by a zero mean and an identity covariance matrix:

$$\mathbf{w} \sim N(\mathbf{0}_p, \sigma_w^2 \mathbf{I}_p), \quad y_n | \mathbf{x}_n = N(\phi(\mathbf{x}_n)^T \mathbf{w}, \sigma_\varepsilon^2) \quad (9)$$

In the above equation, $\mathbf{0}_p$ and \mathbf{I}_p represent the zeros vector and identity matrix, respectively, each with p elements. Meanwhile, σ_w^2 and σ_ε^2 represent the variance terms for the prior of \mathbf{w}

and the independent additive noise, respectively. Defining the regression function $f(\mathbf{x}_n, \mathbf{w}) = E_y\{y|\mathbf{x}_n, \mathbf{w}\}$ yields:

$$f(\mathbf{x}_n, \mathbf{w}) = \phi(\mathbf{x}_n)^T \mathbf{w} \quad (10)$$

$$\mathbf{f}(\mathbf{w}) = [\phi(\mathbf{x}_1)^T \mathbf{w} \quad \phi(\mathbf{x}_2)^T \mathbf{w} \quad \dots \quad \phi(\mathbf{x}_N)^T \mathbf{w}]^T = \Phi(\mathbf{X})\mathbf{w} \quad (11)$$

In the equation above, $\mathbf{X} = \{\mathbf{x}_1 \mathbf{x}_2, \dots \mathbf{x}_N\}$ and $\Phi(\mathbf{X}) \in \mathbb{R}^{N \times p}$. Since \mathbf{f} is a linear function of \mathbf{w} with isotropic Gaussian prior, the following relations can be written [86]:

$$E_{\mathbf{w}}\{\mathbf{f}(\mathbf{w})\} = \mathbf{0}_N \quad (12)$$

$$cov_{\mathbf{w}}(\mathbf{f}(\mathbf{w})) = E_{\mathbf{w}}\{\mathbf{f}(\mathbf{w})\mathbf{f}(\mathbf{w})^T\} = \sigma_w^2 \Phi(\mathbf{X})\Phi(\mathbf{X})^T \quad (13)$$

The inner product between the basis functions, as depicted in the equation above, suggests a kernel definition, such that $k(\mathbf{x}_u, \mathbf{x}_v) = \sigma_w^2 \phi(\mathbf{x}_u)^T \phi(\mathbf{x}_v)$ for any two points \mathbf{x}_u and \mathbf{x}_v in the dataset. This yields $cov(\mathbf{f}) = \mathbf{K}(\mathbf{X})$, where $\mathbf{K}(\mathbf{X}) \in \mathbb{R}^{N \times N}$ is the Gram matrix. From the function-space perspective, any subset of random variables sampled from the GP $f(\mathbf{x})$ has a joint Gaussian distribution with a mean of $m(\mathbf{x})$, that has been taken to be equal to zero in the weight-space perspective discussed above, and a covariance function defined via a kernel $k(\mathbf{x}, \mathbf{x}')$ [87]:

$$f(\mathbf{x}) \sim GP(m(\mathbf{x}), k(\mathbf{x}, \mathbf{x}')) \quad (14)$$

In contrast to the BLR approach, the basis function in GPS is evaluated at an infinite number of points GPR, thereby yielding a nonparametric model. The resulting covariance relation shows that the change of the regression function at different points in feature space, i.e., the covariance, is completely determined by the kernel function defined in the original feature space. This implies that the behavior of the function will be correlated for ‘‘similar’’ points in the original space. Using $n = 1, 2, \dots N$ for the training set and $n = q$ for a test point, the marginal distributions of $\mathbf{y} = [y_1 \ y_2 \ \dots \ y_N]^T$ (also called the evidence function), $\mathbf{y}_{N+1} = [y_1 \ y_2 \ \dots \ y_N \ y_q]^T$ and the conditional distribution of $y_q|\mathbf{y}$ may be determined using matrix normal distribution properties as follows:

$$p(\mathbf{y}|\mathbf{X}) = \int p(\mathbf{y}|\mathbf{f}, \mathbf{X}) p(\mathbf{f}|\mathbf{X}) d\mathbf{f} \sim N(\mathbf{0}_N, \mathbf{C}_N) \text{ with } \mathbf{C}_N = \sigma_\varepsilon^2 \mathbf{I}_N + \mathbf{K}(\mathbf{X}) \quad (15)$$

$$p(\mathbf{y}_{N+1}|\mathbf{X}, x_q) = \int p(\mathbf{y}_{N+1}|\mathbf{f}, \mathbf{X}, x_q) p(\mathbf{f}|\mathbf{X}, x_q) d\mathbf{f} \sim N(\mathbf{0}_{N+1}, \mathbf{C}_{N+1}), \text{ with}$$

$$\mathbf{C}_{N+1} = \begin{bmatrix} \mathbf{C}_N & k(\mathbf{X}, x_q) \\ k(\mathbf{X}, x_q)^T & \sigma_\varepsilon^2 + k(x_q, x_q) \end{bmatrix}_{(N+1) \times (N+1)} \quad (16)$$

$$y_q|\mathbf{y} \sim N(k(\mathbf{X}, x_q)^T \mathbf{C}_N^{-1} \mathbf{y}, \sigma_\varepsilon^2 + k(x_q, x_q) - k(\mathbf{X}, x_q)^T \mathbf{C}_N^{-1} k(\mathbf{X}, x_q)) \quad (17)$$

In the above formulation, \mathbf{C}_N should be positive definite. As a result, the expected value of the response variable at x_q is a linear combination of response variables in the training set weighted with respect to the scaled kernel distance to the query point (67):

$$E\{y_q|x_q, \mathbf{X}, \mathbf{y}\} = f(x_q|\mathbf{X}, \mathbf{y}) = k(\mathbf{X}, x_q)^T \mathbf{C}_N^{-1} \mathbf{y} = \sum_{n=1}^N b_n k(\mathbf{x}_n, x_q) y_n \quad (18)$$

A typical example of a kernel function is the radial basis function (RBF) $k(\mathbf{x}_u, \mathbf{x}_v) = \sigma_f^2 \exp\left(-\frac{\|\mathbf{x}_u - \mathbf{x}_v\|_2^2}{2\sigma_l^2}\right)$, in which σ_f^2 and σ_l^2 denote the variance of the function (signal) and the squared length scale of the kernel, i.e., the range of the influence of the kernel function in the input space. It is possible to determine the optimum values of the kernel parameters, i.e., hyperparameters of the GPR. Using $\boldsymbol{\theta} = [\theta_1 \theta_2 \dots \theta_k]$ as hyperparameters of GPR, e.g., $\boldsymbol{\theta} = [\sigma_f^2 \sigma_l^2]$ for the RBF kernel defined above, one may obtain (using Equation 15) the following log-likelihood:

$$\log p(\mathbf{y}|\boldsymbol{\theta}, \mathbf{X}) = -\frac{1}{2} |\mathbf{C}_N|^{-\frac{1}{2}} \mathbf{y}^T \mathbf{C}_N^{-1} \mathbf{y} - \frac{N}{2} \log 2\pi \quad (19)$$

The function above may be minimized using gradient-based techniques; however, initialization of the hyperparameters is important due to the non-convex nature of the log-likelihood function. Lastly, for a full Bayesian treatment, it is essential to define the priors of $\boldsymbol{\theta}$ and incorporate $\log p(\boldsymbol{\theta})$ into $\log p(\mathbf{y}|\boldsymbol{\theta}, \mathbf{X})$.

Just-In-Time-Learning (JITL)

The development of JITL can be traced back to two seminal studies, in which local weighted regression and instance-based learning were proposed. Contrary to global models that seek to describe data across the entire domain using a single representation, local weighted regression was proposed for approximating nonlinear data over different regions [88]. Similarly, instance-based classification was based on the label of samples similar to the query point, instead of a single decision rule [89]. The accuracy of instance-based predictions for real-valued functions

under realistic conditions was also theoretically justified [90]. These studies merged in JITL (or Lazy Learning) modeling, which has been employed in numerous modeling and process control applications [91–93], including time series analysis [64].

In the context of JITL modeling, the objective is to identify a subset of training points Φ , that exhibits “similarity” to the given query point \mathbf{x}_q consisting of the input features from the entire available historical dataset TS, such that $\Phi \subseteq \text{TS}$. The training of the learner $L(\cdot; \cdot)$ is performed on Φ with the aim of predicting the response for the query point \mathbf{y}_q , given by $\hat{\mathbf{y}}_q = L(\mathbf{x}_q, \Phi)$. This process is repeated for each query point, and the decision of whether to concatenate the predicted query point (along with its real or predicted response variable value) to TS is application-dependent. The key to obtaining accurate predictions via JITL lies in the procedure of selecting the relevant subset. Typically, proximity in feature space, as measured by Euclidian distance between feature values, has been used to determine the similarity of observations. The k -neighbors of each query point (k usually determined by a validation set) are determined as the k -observations with the smallest Euclidian distance to the query point [91]. However, the efficacy of this criterion is contingent on the learner and the data environment. For instance, a (weighted) linear regression may be preferred over more advanced learning methods for small k values, since it would be difficult to train the latter using a small sized Φ due to a presumable high capacity. As another example, MW modeling is usually used to adapt to the most recent operating conditions, and MW can be classified as a type of JITL method, in which relevant data is selected not in relation to proximity in feature space, but rather to proximity to sampling time. Consequently, various methods for instance selection have been proposed in the literature on soft-sensors [63,94–96]. In the present study, proximity on a 2-D grid comprised of years and months is adopted as the similarity measure. A relevant subset of the training set is selected to span W_y years and W_m months prior to the year and month of the query point, respectively (see Section 4.2 for details). In this context, the hyperparameters W_y and W_m , which are instrumental in determining the size of the local training set, are tuned using rolling-origin forecasting in the training set, starting from a buffer period of 48 observations.

Metrics for Assessing Prediction Accuracy

In the context of validating and selecting the most suitable models, as well as for parameter tuning (i.e., model fit), comparing alternative models, and evaluating the overall forecast performance [97], the most frequently used performance measures are the root mean square

error (RMSE), the mean absolute error (MAE), and the mean absolute percentage error (MAPE).

Equations 20-22 present the formulae of these performance measures, where y_i represents the actual values, \hat{y}_i denotes the predicted values, and n corresponds to the number of observations in the dataset. For a more in-depth exploration of additional performance measures, readers are encouraged to refer to the works of [98] and [99].

$$\text{MAE} = \frac{1}{n} \sum_{i=1}^n |y_i - \hat{y}_i| \quad (20)$$

$$\text{RMSE} = \sqrt{\frac{\sum_{i=1}^n (y_i - \hat{y}_i)^2}{n}} \quad (21)$$

$$\text{MAPE} = \frac{100}{n} \sum_{i=1}^n \left| \frac{y_i - \hat{y}_i}{y_i} \right| \quad (22)$$

DATA DESCRIPTION

The tariff methodology is instrumental in determining the revenues of natural gas distribution companies with regulated tariffs by calculating the System Usage Fee (SUF) based on consumption levels. A tariff period is set to last five years, during which SUF is calculated at the beginning based on past realizations using statistical models as follows: $SUF = \text{Revenue Requirement (OPEX + CAPEX)} / \text{Total Consumption}$, where OPEX stands for operating expenses and CAPEX stands for capital expenditures.

Accurate natural gas consumption estimates are critical for regulated companies, as deviations in five-year estimates can lead to unexpected income losses or gains due to regulatory revisions. While OPEX and CAPEX transfers are mathematically predictable, external and environmental factors complicate long- and short-term consumption forecasts. Advanced modeling techniques and data analysis methods are used to improve these estimates, but monthly accuracy remains challenging. Enhancing natural gas consumption forecasts is strategically vital for efficient resource management in the natural gas distribution sector.

The existing dataset, provided by SOCAR, consists of monthly residential NGD consumption in million standard m^3 (msm^3) in Bursa and Kayseri from January 2014 to August 2024. This dataset was divided into a training/validation set of 108 observations (9 full years) between 2014 and 2022 and a test set of 19 observations (1 year and 7 months) between 2023 and 2024. The former set was used for building models and tuning the hyperparameters, while the latter was exclusively used for giving unbiased test set performance, similar to the monthly NGDP values for a one-year-period, as stipulated by the company. The NG consumption is ascertained through the monitoring of local sensors situated in residential areas and buildings. It was reported by SOCAR that the summer period readings, i.e., July, August and September in Bursa, and June, July, August and September in Kayseri, during 2014 to 2019, were not conducted exactly on time; the readings for the first two months were delayed, and the last months' readings included some of the consumption of the prior months. Consequently, the Results section details the correction of summer period data in the training set prior to forecasting. The construction of time series and JITL-GPR models was then executed using the corrected training dataset. Figures 1 and 2 below illustrate depict the logarithmically transformed time series of NG consumption, in addition to its primary components, for Bursa and Kayseri, respectively. A visual examination of these plots indicates the presence of trend and additive seasonality in the datasets of both cities.

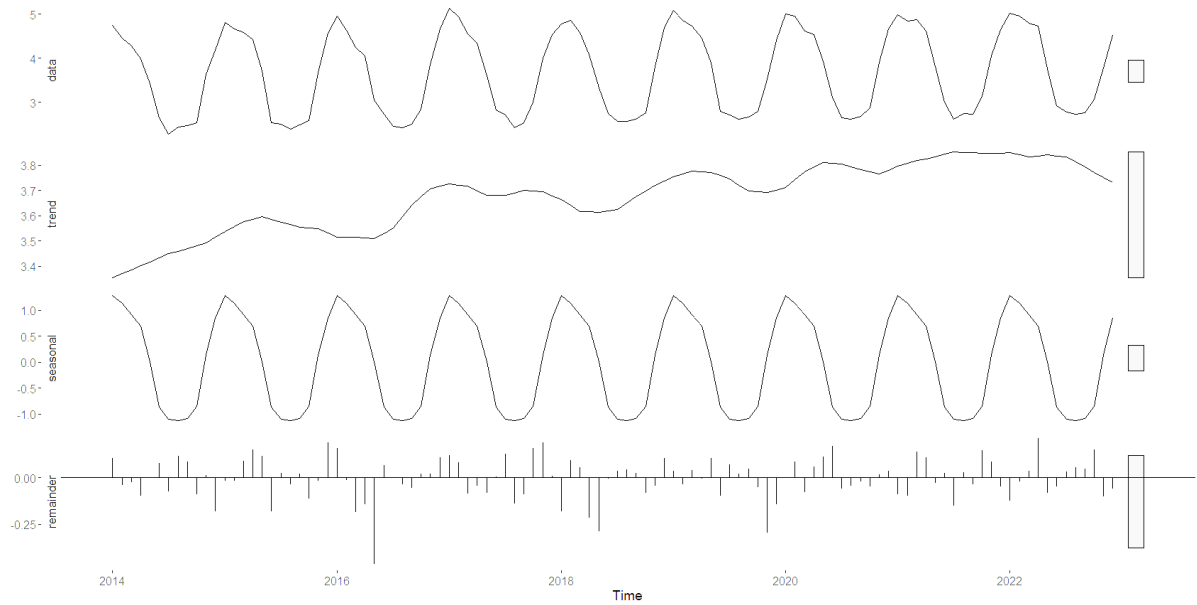


Figure 1. The STL decomposition of the logarithm of Bursa's corrected NG consumption data (January 2014 to December 2022).

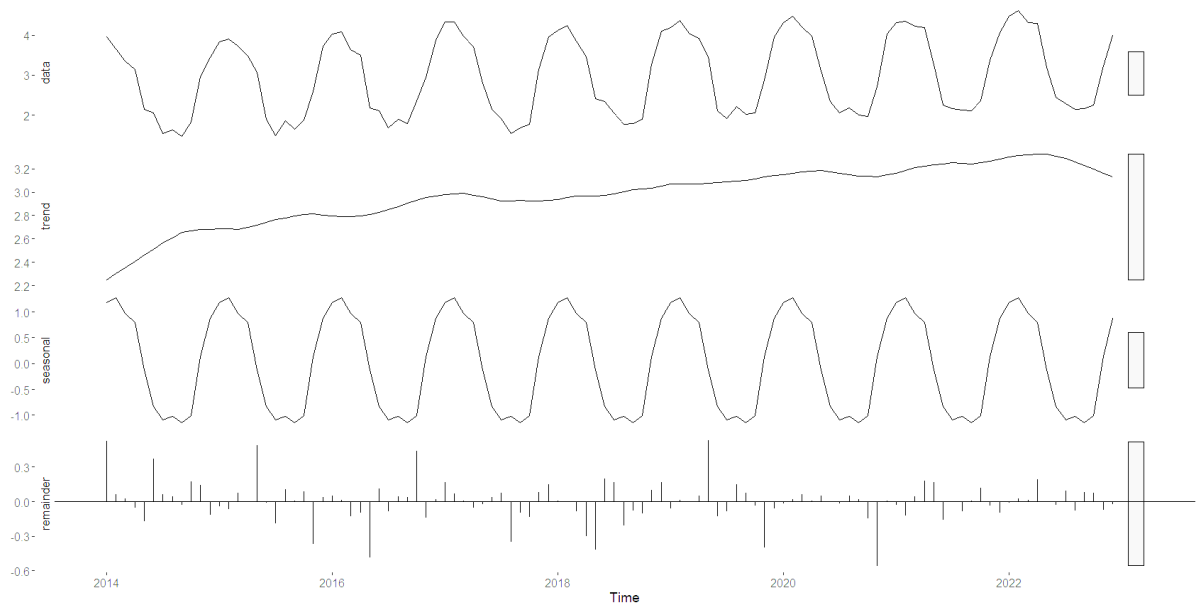


Figure 2. The STL decomposition of the logarithm of Kayseri's corrected NG consumption data (January 2014 to December 2022).

RESULTS AND DISCUSSION

Correction of NGD Data during Summer Season

For the correction of NGD values in these months, a linear model is proposed:

$$D_{y,m} = T_{y,m} + R_{y,m} + e_{y,m} \quad (23)$$

Here, $D_{y,m}$ denotes the demand observed in the y^{th} year and m^{th} month; $T_{y,m}$ is the long-term effect on demand, to be extracted from the annual trend for the m^{th} month. The second additive term, which is assumed to be orthogonal to the first, is $R_{y,m}$, which denotes the short-time effect, to be extracted from NGD in the recent months, and the last term is the unpredictable zero-mean error term. Trend estimates can be obtained by employing simple linear regression on $D_{y,m}$ vs. year data for each month since a single global fit (to untransformed NGD) seems to be a poor fit for all the months (Figure 3A):

$$\widehat{D}_{y,m} = T_{y,m} = \hat{\beta}_{0m} + \hat{\beta}_{1m}y \quad (24)$$

It is assumed that there exists (at least) lag-1 (one month) correlation between $D_{y,m}$ values for successive months, stemming from $R_{y,m}$ terms, i.e., $\text{Corr}(R_{y,m-1}, R_{y,m})$. Noting that $R_{y,m} + e_{y,m} = D_{y,m} - T_{y,m}$, and the random error terms are independent, the lag-1 correlation can be estimated from $\text{Corr}(\mathbf{D}_{m-1} - \mathbf{T}_{m-1}, \mathbf{D}_m - \mathbf{T}_m)$ using $\mathbf{D}_m = [D_{1,m} \ D_{2,m} \ \dots \ D_{9,m}]^T$ and $\mathbf{T}_m = [T_{1,m} \ T_{2,m} \ \dots \ T_{9,m}]^T$ for the m^{th} month (see Text S1 in Supporting Materials for more information). In the light of the above modeling perspective, the correction procedure of NGD values during the summer season for six successive years, yielding $6 \times 3 = 18$, and $6 \times 4 = 24$ data points for Bursa and Kayseri, respectively, is formulated as an optimization problem. Given monthly NGD data for nine years in \mathbf{D}_m , $m=1, 2, \dots, 12$, it is desired to replace $D_{y,m}$ with $y = 1, 2, \dots, 6$ and $m = m_0, m_0 + 1, \dots, 9$ (m_0 is taken to be 7 and 6 for Bursa and Kayseri, respectively) with the optimum $\mathbf{D}_c = \{D_{y,m}^c; y = 1, 2, \dots, 6; m = m_0, m_0 + 1, \dots, 9\}$ values (c stands for corrected data), resulting in $\mathbf{D}_m^c = [D_{1,m}^c \ D_{2,m}^c \ \dots \ D_{6,m}^c \ D_{7,m} \ D_{8,m} \ D_{9,m}]^T$ (note that the last three $D_{y,m}$ values are correct readings and are therefore treated as constants). Defining $\Phi =$

$$\begin{bmatrix} 1 & 1 \\ 1 & 2 \\ \vdots & \vdots \\ 1 & 9 \end{bmatrix}_{9 \times 2}, \text{ the following objective function is proposed for minimization (see Text S2 for more}$$

detailed information about the optimization function and the accompanying constraints):

$$\Psi(\mathbf{D}_c) = - \left\{ \sum_{m=m_0}^9 \text{corr}(\mathbf{D}_m^c, \mathbf{T}_m) / (9 - m_0 + 1) + \sum_{m=m_0}^{10} |\text{corr}(\mathbf{D}_{m-1}^c - \mathbf{T}_{m-1}, \mathbf{D}_m^c - \mathbf{T}_m)| / (10 - m_0 + 1) \right\} \quad (25)$$

where $\mathbf{T}_m = \Phi(\Phi^T \Phi)^{-1} \Phi^T \mathbf{D}_m^c = \mathbf{H} \mathbf{D}_m^c$ for $m=m_0, m_0 + 1, \dots, 9$, and $\mathbf{T}_m = \mathbf{H} \mathbf{D}_m$ otherwise, subject to the following constraints:

$$\sum_{m=m_0}^9 D_{y,m}^c = \sum_{m=m_0}^9 D_{y,m}, y = 1, 2 \dots 6 \quad (26)$$

$$D_{y,m}^c \geq 0, y = 1, 2, \dots, 6; m = m_0, m_0 + 1, \dots, 9 \quad (27)$$

The optimization was performed with *fmincon* in the Optimization Function of MATLABTM using the interior-point method [100] with the initial parameter values, i.e., the monthly NGD values during the summer period, all assumed to be equal to 10 msm³, slightly lower than the actual readings obtained during the last three years. The results of the optimization are shown in Figure 3B-D for Bursa. In addition, Figs. 3E-F show that the irregular behavior during the summer season seen in the original time series has been corrected for both cities.

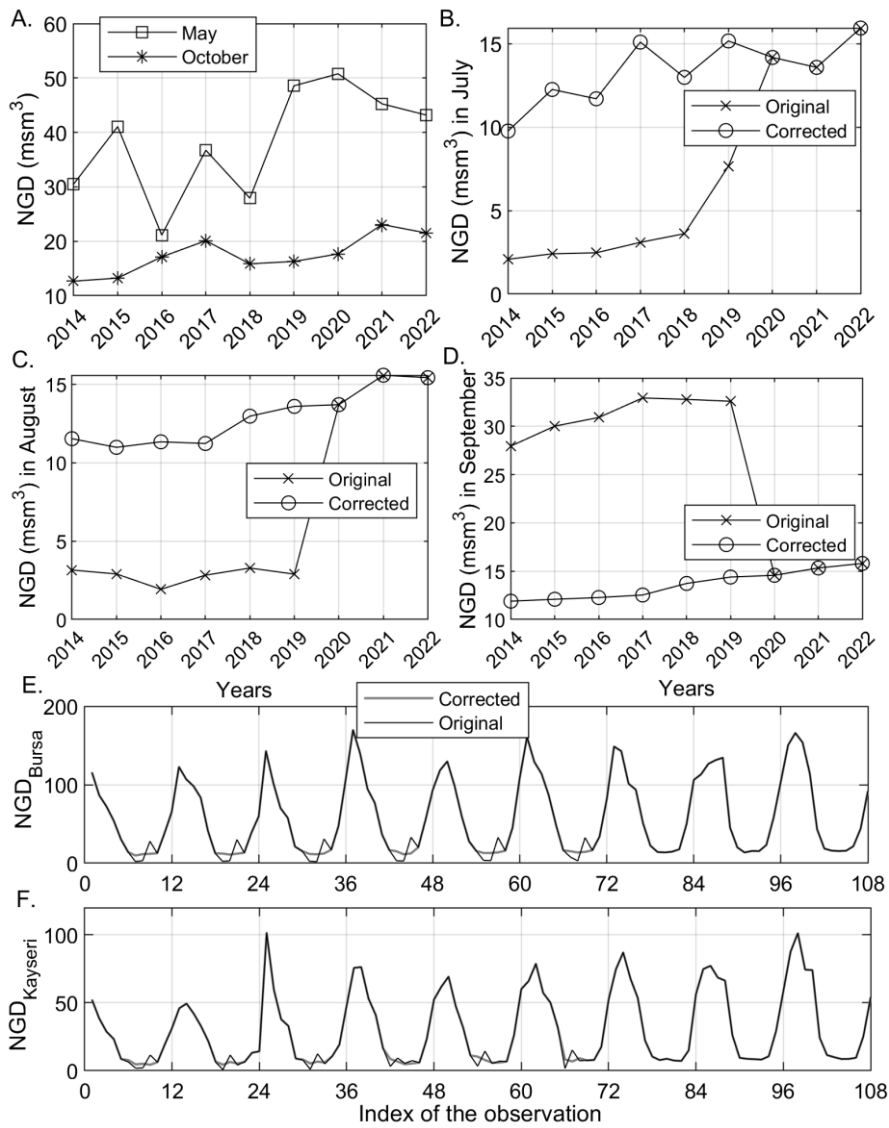


Figure 3. (A) NGD values in Bursa for May and October over 2014-2022. The original and corrected NGD values in Bursa for (B) July, (C) August, and (D) September 2014-2022. The original and corrected (“smoothed” gray lines during the summer periods in the figures) monthly NGD values in the training sets of (E) Bursa and (F) Kayseri.

Time Series Modeling

Outliers were identified in both “corrected” datasets: five in the training set for Bursa and two for Kayseri. During the modeling process, cases in which these values were not smoothed and cases in which they were smoothed were treated separately. Both datasets indicated the utility of a logarithmic transformation; therefore, models were constructed separately for the original data and the transformed data. In light of the observed trend and seasonality in the data, we produced forecasts using four primary statistical models as a benchmark for the proposed approach: STL, SARIMA, ETS, and TBATS. We also implemented a machine learning-based

combination technique, the AI-AFTER algorithm. The elapsed time for forecasting did not exceed 25 seconds in any case. The models were constructed using the training set, and the estimated parameters were subsequently applied to the validation data. As the performance of the models on the training and validation sets did not exhibit any anomalies, there was no necessity to update the parameters. All of the model orders were verified in several in-sample forecasting trials. Table 2 below provides descriptions of some of the models considered in this study. Once the model parameters were estimated using the training sample, 19-step-ahead forecasts were produced by the candidate models to evaluate their post-sample performances.

Table 2. Details on the time series models applied to the logarithms of the corrected NG data

Abbreviation	City	Description and References
ETS	Bursa	Additive Holt-Winters' Method with multiplicative errors and parameters $\alpha = 0.00113$, $\beta = 0.00010$, and $\gamma = 0.00011$.
	Kayseri	Additive Holt-Winters' Method with additive errors and parameters $\alpha = 0.00290$, $\beta = 0.00289$, and $\gamma = 0.00013$.
SARIMA	Bursa	Seasonal Autoregressive Integrated Moving Average model with drift, designated as $p = 1$, $d = 0$, $q = 0$; $P = 2$, $D = 1$, $Q = 0$.
	Kayseri	Seasonal Autoregressive Integrated Moving Average model with drift, designated as $p = 1$, $d = 0$, $q = 0$; $P = 0$, $D = 1$, $Q = 1$.
STL	Bursa	The data for both cities was subjected to additive seasonality with parameters s.window = "periodic" and t.window = 13, and robust fitting was adopted in the LOESS procedure.
	Kayseri	
TBATS	Bursa	Omega, the Box-Cox parameter = 0.91; ARMA(1,0) model was fitted; no damping; # of seasonal periods = 12; # of Fourier terms used for each seasonality = 4.
	Kayseri	Omega, the Box-Cox parameter = 1.00; ARMA(0,0) model was fitted; no damping; # of seasonal periods = 12; # of Fourier terms used for each seasonality = 5.

The predictive performances of the time series models examined in this study are evaluated using the accuracy metrics provided in Equations 20-22. TBATS and the AI-AFTER algorithm exhibited superior performance in comparison to the other models for Bursa and Kayseri, respectively, as illustrated in Table 3. It must be noted that the initial 35 observations in the training set were used to train the candidate forecasts by the AI-AFTER algorithm, and were consequently not accessible to the analyst. Thus, the performance metrics of this method on the Kayseri training set were determined using a total of 73 observations, rather than 108.

Table 3. Accuracy metrics for the benchmark time series model on the training and test sets.

City	Bursa					Kayseri				
	SARIMA	ETS	STL	TBATS	AI-AFTER	SARIMA	ETS	STL	TBATS	AI-AFTER
RMSE _{1-step} (msm ³)	9.212	9.569	9.366	9.024	8.863	5.383	5.120	5.956	5.221	5.275
MAE _{1-step} (msm ³)	5.917	6.185	6.300	6.355	6.023	3.593	3.409	3.888	3.446	3.657
MAPE _{1-step} (%)	10.43	10.02	11.40	11.08	9.39	13.21	13.53	16.86	13.19	12.59
RMSE _{test} (msm ³)	19.221	20.361	19.566	14.857	16.751	10.778	8.286	9.013	6.786	6.332
MAE _{test} (msm ³)	14.367	13.244	14.211	9.666	11.208	7.822	5.828	7.189	5.094	4.140
MAPE _{test} (%)	19.79	18.34	20.74	14.24	15.60	18.21	14.62	20.12	13.26	11.87
NGD in 2023 (msm ³)	816.8	816.8	816.8	816.8	816.8	477.6	477.6	477.6	477.6	477.6
NGD in 2023 prediction (msm ³)	850.9	867.7	690.8	779.3	797.9	519.7	502.1	401.6	451.0	475.4
Yearly PE in 2023	4.18	6.23	-15.42	-4.58	-2.31	8.83	5.15	-15.90	-5.55	-0.45

Figures 4 and 5 illustrate the training and test data (black lines), and the predictions (blue lines) and forecasts (red dashed lines) generated by the TBATS model for Bursa and the AI-AFTER algorithm for Kayseri, respectively. Finally, Figures 6 and 7 demonstrate how well the standardized residuals from each of these two models fit to a proper normal distribution. While three of the residuals generated by the TBATS model are potential outliers, the number of such cases is two for the AI-AFTER algorithm. However, the Ljung-Box test statistic was found insignificant at lag 4 in both cases ($Q = 3.092$ for Bursa and $Q = 4.362$ for Kayseri), indicating that autocorrelation in the residuals is not an issue at $\alpha = 0.05$.

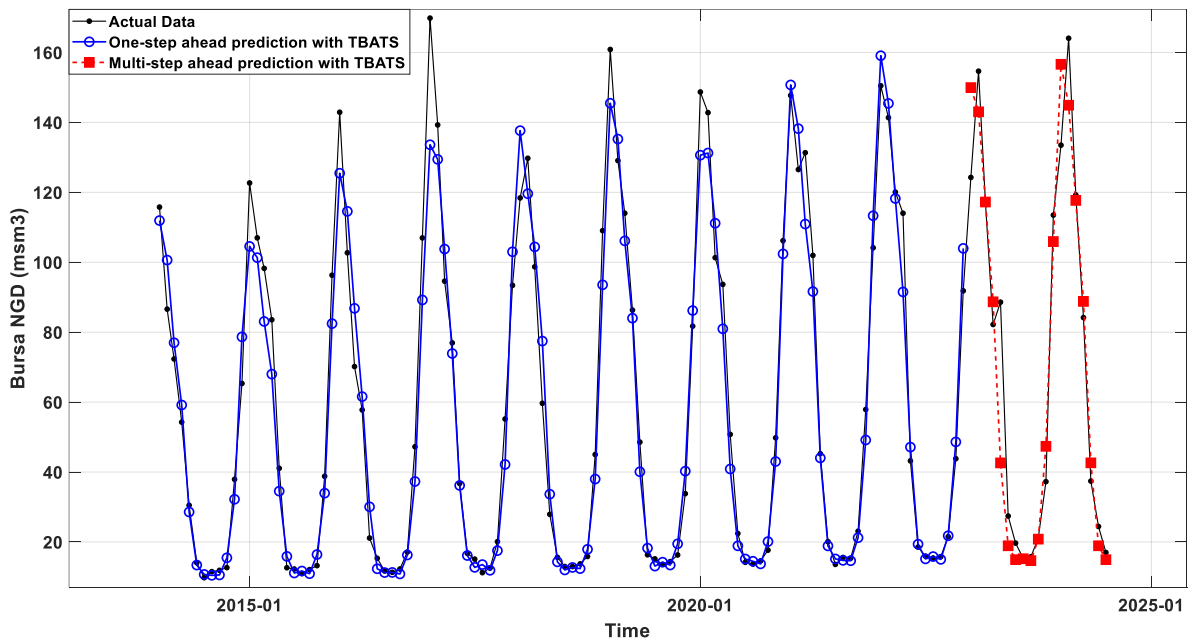


Figure 4. The real NGD values, one-step ahead training set predictions, and multi-step ahead test set predictions using the TBATS model for Bursa.

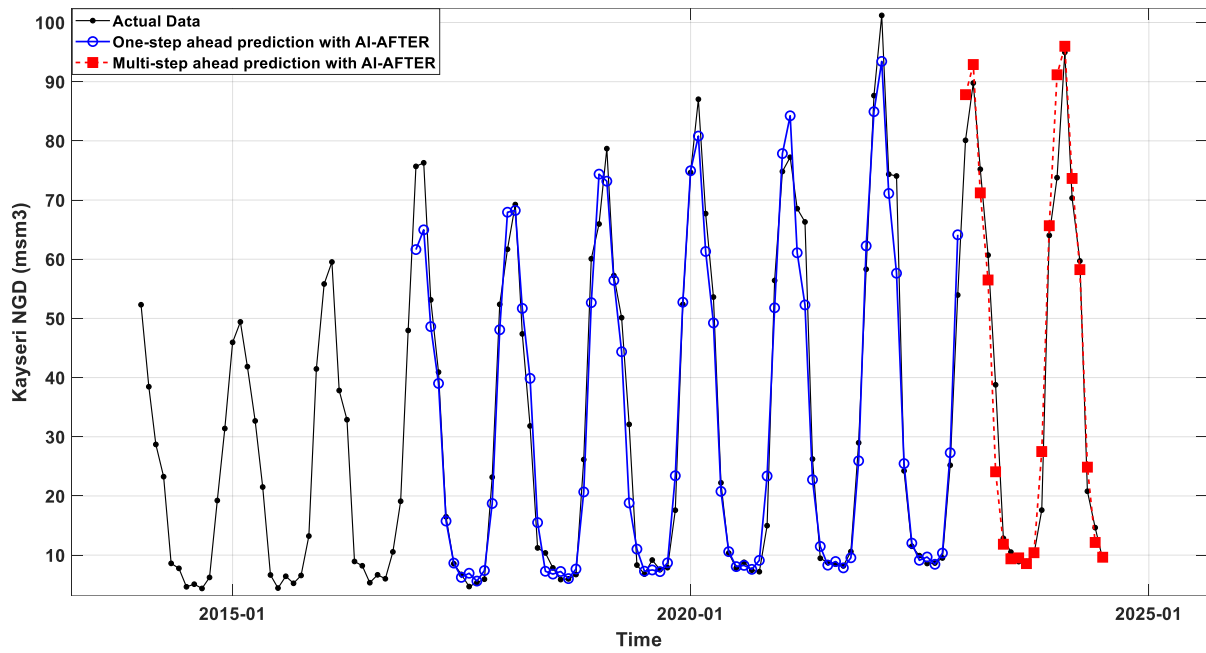


Figure 5. The real NGD values, one-step ahead training set predictions, and multi-step ahead test set predictions using the AI-AFTER algorithm for Kayseri.

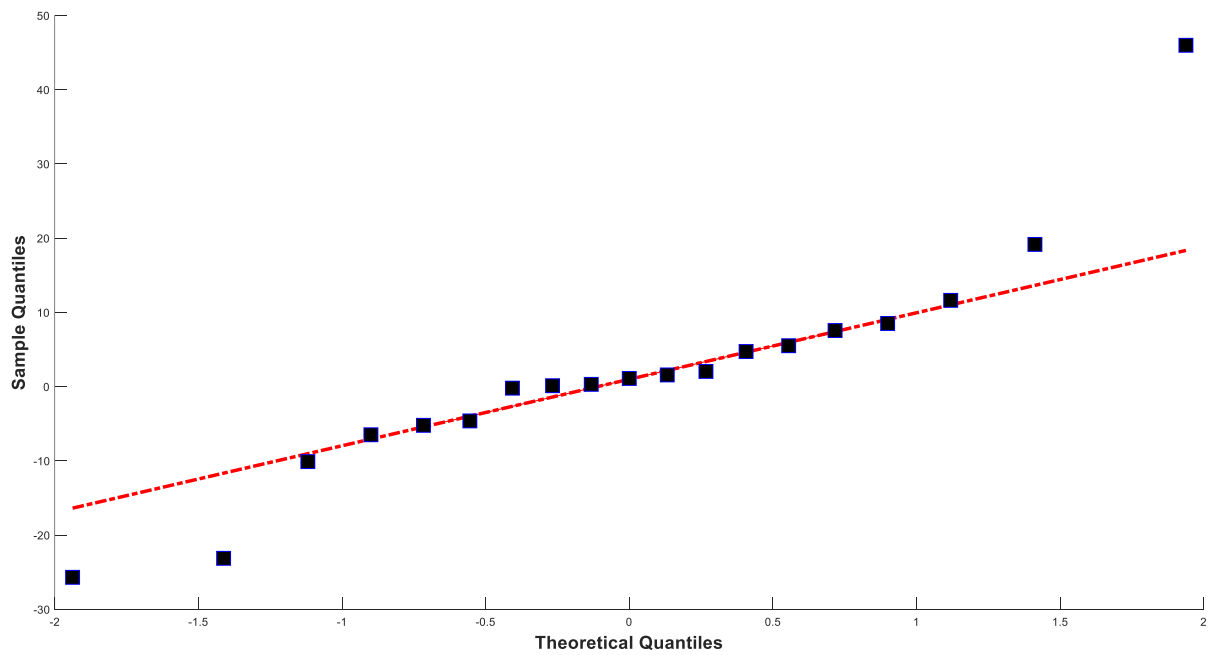


Figure 6. QQ Plot for the multi-step ahead test set prediction residuals for Bursa.

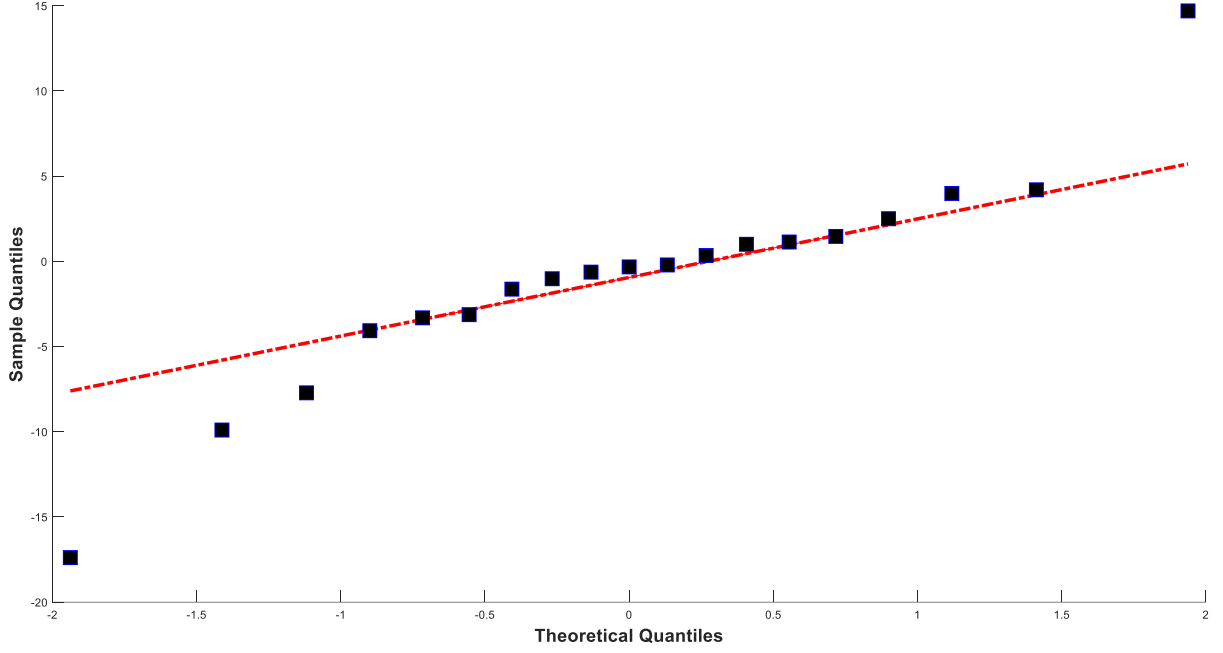


Figure 7. QQ Plot for the multi-step ahead test set prediction residuals for Kayseri.

JITL-GPR Modeling

The JITL-GPR forecasting method consists of two steps: (i) selecting a convenient subset of training set, i.e., the local training set, for each query point, and (ii) applying GPR to the local training set and predicting the query point.

Local subset selection

In the traditional time series representation for regression in NGDP, including the studies using machine learning tools, the features (excluding exogenous variables) correspond to the response variable sampled at previous time lags [23,59,101]:

$$\hat{D}_{t+1} = f(\mathbf{x}_t), \quad \mathbf{x}_t = [D_t \ D_{t-1} \ \dots \ D_{t-p+1}]^T \in \mathbb{R}^p \quad (28)$$

In the present study, however, a different feature representation is adopted. The input features are assumed to be year and month values, i.e., $y = 1, 2, \dots, n_T$; $m = 1, 2, \dots, 12$, and for each point on this two-dimensional (2-D) grid, similar to a 2-D Gaussian random field, the NGD value $D_{y,m}$ is taken to be the response variable. Thus, the training (historical) dataset is defined as $TS = \{(y, m, D_{y,m}); y = 1, 2, \dots, n_T; m = 1, 2, \dots, 12\}$. To predict the future query points (test set), a data segment with convenient window widths (W_y, W_m), representing the number of previous years and months, respectively, is extracted from the historical dataset, and GPR is employed on this 2-D data window. This procedure is to be repeated for all query points, thereby

rendering the proposed method an application of JITL. It is to be noted that the similarity of the query point to the training data is based on proximity in years and months (on the 2-D grid), and is computed using modular arithmetic. In other words, the month indices 1 (January) and 12 (December) in two successive years are assumed to be in close proximity, similar to the rationale in time series analysis. Thus, for a query point with the index $q = 12y + m$, in which y and m values are known, the following function $\Phi(T, q, W_y, W_m)$ is used to extract the relevant subset from the training dataset TS with the help of an accompanying function $f(n)$, which extracts year, month and NGD value of the $(n - 1)^{th}$ observation via $f(n) = (\text{ceil}((n - 1)/12), \text{mod}(n - 2, 12) + 1, D(n - 1))$:

$$\begin{aligned} \Phi(T, q, W_y, W_m) = \{f(n) = (y, m, D_{y,m}), n \in \{1, 2, \dots, q\}\} = \\ \{f(q), f(q - 1), \dots, f(q - W_m + 1), f(q - 11), f(q - 12), \dots, f(q - 11 - (W_m - 1)), \dots \\ f(q - (n \times 12 - 1)), f(q - n \times 12), \dots, f(q - (n \times 12 - 1 - (W_m - 1))), \dots, \\ f(q - ((W_y - 1) \times 12 - 1)), \dots, f(q - ((W_y - 1) \times 12 - 1 - (W_m + 1)))\} \quad (29) \end{aligned}$$

In the equation above, $\text{ceil}()$ and $\text{mod}()$ are ceiling and mod functions, respectively. While a quick look at Equation 29 gives the impression of a rather complicated local dataset construction method, it is indeed quite simple. As an example, the construction of the local training set for the first query point in the test set (the 109th point, January 2023) is demonstrated for $W_y = 4$ and $W_m = 3$. Table 4 shows the years and months of the data in the TS in 2-D grid form, and NGD values (in time-index format) are placed in each corresponding cell. The query point in the 11th year is shown with a dark gray cell, where D_q is unknown. Since $W_m = 3$, the last three months, including the query month, are included in the local training set, hence D_{106} and D_{107} , corresponding to November and December of 2022, are selected (in light gray color). For one-year lagged observations, NGD values for November 2021, December 2021, and January 2022 are selected, corresponding to D_{95} , D_{96} , and D_{97} , respectively. This selection method is repeated to include observations up to W_y years, which corresponds to the selection method proposed in Equation 29. In this way, the historical samples that are similar to the current query point in terms of the seasons are selected. To construct the local training set for the next query point (110th point, February 2024), the same procedure is repeated using the W_y and W_m values for February, while the already predicted value for January is used as a training set point. Thus, multi-step-ahead forecasting is achieved in an iterative manner.

Table 4. An example of how a local training set is selected in JITL-GPR model.

Years/ Months	1	2	...	7	8	9	10	11
1	D_1	D_{13}	...	D_{73}	D_{85}	D_{85}	D_{97}	$D_q=D_{109}$
2	D_2	D_{14}	...	D_{74}	D_{86}	D_{86}	D_{98}	
...	
10	D_{10}	D_{22}	...	D_{82}	D_{94}	D_{94}	D_{106}	
11	D_{11}	D_{23}	...	D_{83}	D_{95}	D_{95}	D_{107}	
12	D_{12}	D_{24}	...	D_{84}	D_{96}	D_{96}	D_{108}	

The k^{th} element of the (y, m) pair in the subset extracted by $\Phi(T, q, W_y, W_m)$ is denoted by \mathbf{x}_k , i.e., $\Phi(T, q, W_y, W_m) = \{(\mathbf{x}_k, D_k), k = \{1, 2, \dots, W_y \times W_m - 1\}\}$; furthermore, $\mathbf{X}_{JITL} = \{\mathbf{x}_k, k = \{1, 2, \dots, W_y \times W_m - 1\}\}$ and $\mathbf{D}_{JITL} = \{D_k, k = \{1, 2, \dots, W_y \times W_m - 1\}\}$ are used for ease of representation. For a given query point \mathbf{x}_q , \mathbf{X}_{JITL} and \mathbf{D}_{JITL} are determined and z-score scaled. Finally, GPR is used (see Equation 18) to determine the expected value of NGD at the query point, $E\{D_q | \mathbf{x}_q, \mathbf{X}, \mathbf{D}_{JITL}\} = f(\mathbf{x}_q | \mathbf{X}_{JITL}, \mathbf{D}_{JITL})$ (please note that the symbol y used in Sections 2.1 and 2.2 for the output variable is now reserved for the feature year number) using the *fitgrp* function in the Statistics and Machine Learning Toolbox of MATLAB™.

Kernel Design

Based on the observation that NGD values exhibit a nearly linear trend in the long-run, with sinusoidal-like behavior within each year, an additive kernel that consists of a homogeneous linear kernel for years and a second order polynomial kernel for months is designed. Given two vectors $\mathbf{x}_u = [y_u \ m_u]^T$ and $\mathbf{x}_v = [y_v \ m_v]^T$, with $u, v \in \{1, 2, \dots\}$, index of the observation, two basic kernels are added to form a convenient kernel function.

$$k(\mathbf{x}_u, \mathbf{x}_v) = \sigma_f^2 (\beta^2 y_u^T y_v + (m_u^T m_v + \alpha^2)^2) \quad (30)$$

The three hyperparameters in GPR, σ_f^2 , β^2 , and α^2 , are expected to adjust the variance of the response variable, the weight of the “year effect” relative to the “month effect” (or scale parameter), and the curvature of the NGD in recent months. These three hyperparameters were all initialized with unity in the optimization of marginal loglikelihood, since all variables were z-normalized, and identical results were obtained using initial values between 0.2 and 5. Finally, the mean of the GPR function (see Equation 14) was set equal to zero, i.e., no fixed basis functions were used.

Window size tuning

To adjust the hyper-parameters of the JITL-GPR model, the first 48 observations in the TS were reserved as a “buffer” region, and observations with indices 49 to 108 (60 data points) in the TS were predicted using a moving horizon estimation method, i.e., once a query point is predicted, it is included in the training set accessible for the next query sample. Here, a grid search over the local dataset window sizes of $W_y = \{2, 3, \dots 8\}$ and $W_m = \{2, 3, \dots 6\}$ (see Text S3 for the rationale of selecting these ranges for the hyperparameters) is performed to find a single (W_y, W_m) parameter pair (applicable to all query points) with the smallest one-step-ahead RMSE value. Using this method on Bursa yielded an RMSE of 14.1 msm^3 at $(W_y, W_m) = (8, 3)$; however, a surface plot of RMSE values over all the parameter value combinations showed that $\text{RMSE} \leq 15.5 \text{ msm}^3$ was obtained for all W_m values and $W_y \geq 4$ (figure not shown). This indicated that the prediction accuracy did not change with respect to the number of previous months included in the model as long as more than four successive years of data were included. This was indeed unexpected; hence we examined the phenomena in more detail. We grouped 60 predictions into 12 groups of five observations (years) each, and found that the RMSE surfaces with respect to parameter values changed significantly from month to month. This indicated that the flat RMSE surface with respect to window sizes is due to an “averaging out” effect over 12-months, i.e., using the same window size for all months yields an inferior and almost constant performance over a range of window sizes.

Due to the limited number of historical observations, with each month having only five observations available for tuning the window size, it is not feasible to tune a separate (W_y, W_m) pair for each month. Combining “similar” months into single units is a better strategy, which has been frequently employed in the NGDP literature for predictive purposes [5,9]. To this end, the similarity of RMSE surfaces with respect to parameter values for all pairs of successive months was checked and series of similar months were grouped together (Text S4 and Figure S1). Consequently, All NGD values during January-May (five months), June-September (four months), and October-December (three months) are grouped as Group I, Group II and Group III, respectively.

Predictions of JITL-GPR for the Test Set

For each group, which now contained 25, 20, and 15 observations, (W_y, W_m) parameter values that yield the minimum RMSE, were found to be equal to 13.22 msm^3 ($\sim 1 \text{ msm}^3$ smaller than the previous value), were determined. The results for the two cities are shown in Table 5. It is

interesting to note that the optimum values of the window parameters show a striking similarity for both cities, indicating a more general NGD tendency that is not localized to a specific location. The optimal value of W_y varies less between the groups compared to that of W_m ; only the NGD at the beginning of winter (Group III) seems to be less affected by the slow annual trend, but related to the very recent demand values. The information of the previous months was found to be more important for the months with higher heating demand. We can speculate that this information could be helpful for the GPR model in determining the recent trend in weather and economic conditions that affect the heating habits of the residents.

Table 5. W_y, W_m values that yield the minimum RMSE values of one-step ahead predictions

City	Bursa			Kayseri		
Groups	I	II	III	I	II	III
Optimum W_y	8	8	5	8	8	2
Optimum W_m	6	2	4	6	2	4

Two examples of multi-step-ahead predictions for the test set of Kayseri are demonstrated in Figures 8A and 8B for January (one-step-ahead) and November (11-step-ahead) 2023, respectively. Note that $\{W_y, W_m\}$ pair is taken to be equal to $\{8, 6\}$ for January, and $\{2, 4\}$ for November (see Table 5). Here, the 0th year corresponds to the query time and the W_m-1 months before it, so the year is not taken as an absolute time measure. In both figures, the GPR surfaces fit the historical data well, and predict the test point quite accurately. Table 6 shows that the accuracy of the JITL-GPR predictions for the test set exceeds that of the time-series models; moreover, the percentage error of the prediction of the total NGD in 2023 is less than 1% for both cities, indicating that the government regulations for annual predictions are satisfactorily met. A comparison of the results of JITL-GPR with those from time series methods, as presented in Section 4.2, indicates that the JITL-GPR approach led to a reduction in out-of-sample RMSE values by 14.6% for Bursa and 19.3% for Kayseri, as well as a decrease in MAE values by 2.5% for Bursa and 10.4% for Kayseri (see Figure 9). The proposed model led to a 5.1% reduction in MAPE for Bursa, yet it did not achieve the same outcome for Kayseri. Figure 10 shows one-step ahead predictions for the training set and the multi-step ahead predictions for the test set for both cities, again indicating that the forecasts adequately follow the actual demand values. Finally, the prediction residuals, defined as the difference between the predicted and actual NGD values, generally show a similar picture for both cities (see Figure 11). Overpredicted NGD values in the first year may be due to small number of historical data (only

the first four years of data are available to predict the 49th observation), especially to accurately determine the annual trend, while underpredicted NGD values in the winter of 2021-2022 (observations #95-100) may be due to a concept drift, such as economic conditions imposed by the COVID pandemic. However, the advantage of using an adaptive JITL mechanism is seen here; the inclusion of these “unexpected” NGD values within the window of the JITL-GPR leads to more accurate predictions of the next year’s NGDPs.

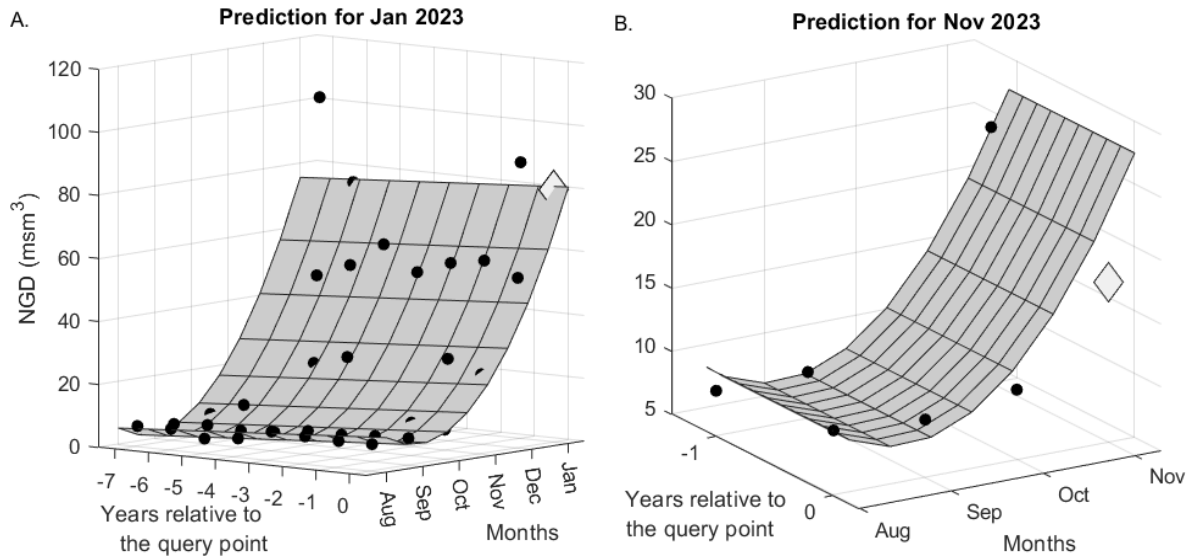


Figure 8. NGDP for (A) January, and (B) November 2023. The filled circles represent the training sets in both subfigures, and also NGDPs for August-October 2023 (in the left subfigure); while the large diamonds denote the true value of the query point.

Table 6. Accuracy metrics for the JITL-GPR model on the training and test sets.

City	Bursa	Kayseri
RMSE_{1-step} (m³)	13.23	6.407
MAE_{1-step} (m³)	8.485	4.590
MAPE_{1-step} (%)	12.20	16.34
RMSE_{test} (m³)	12.69	5.110
MAE_{test} (m³)	9.424	3.711
MAPE_{test} (%)	13.51	14.63
NGD in 2023 (m³)	816.8	477.6
NGD in 2023 prediction (m³)	824.3	473.6
Yearly PE in 2023	0.90	-0.83

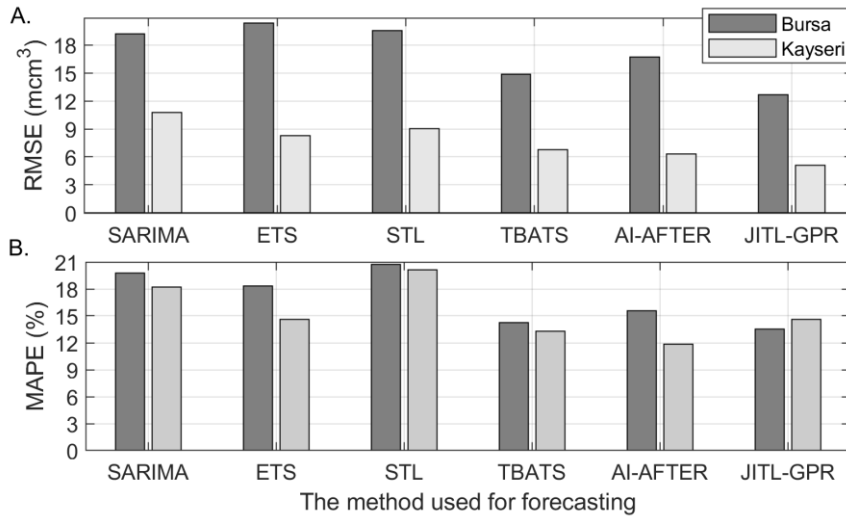


Figure 9. Comparison of RMSE and MAPE values of different methods for the test set.

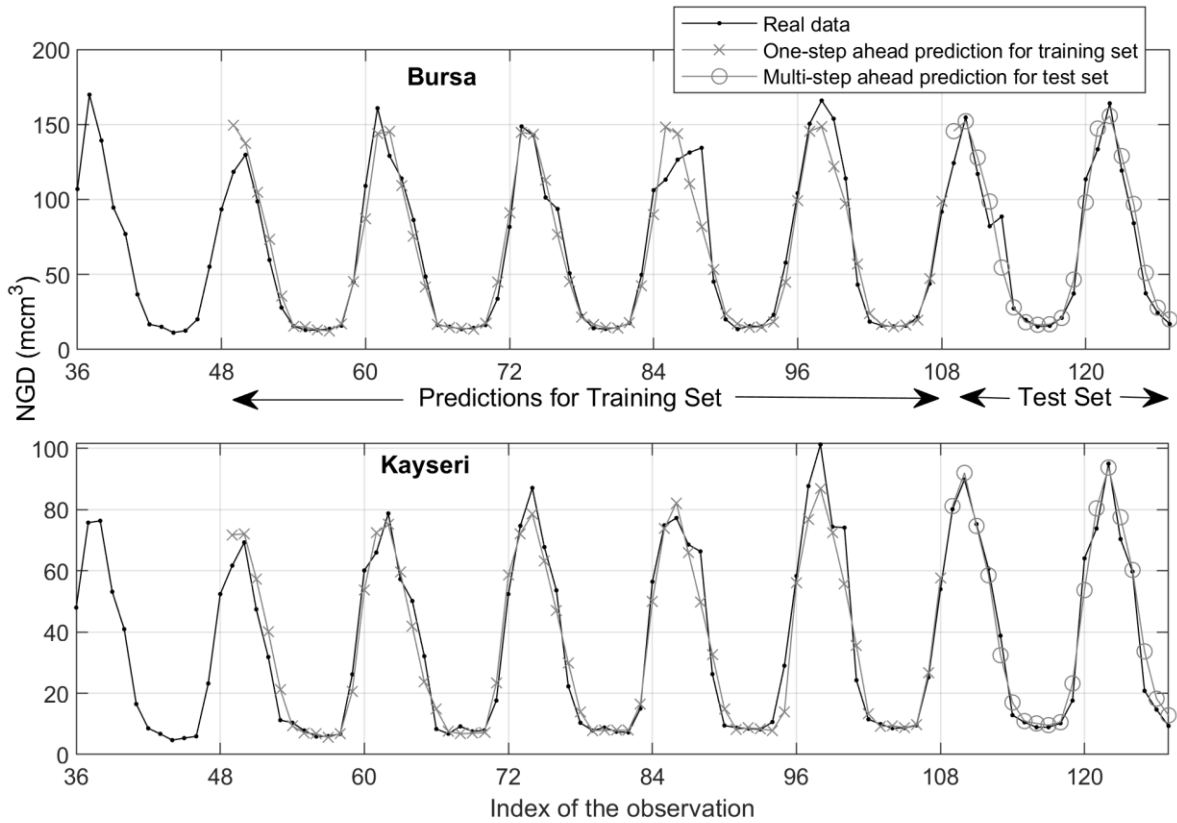


Figure 10. Comparison of real, one-step ahead training set and multi-step ahead test set predictions of NGD values.

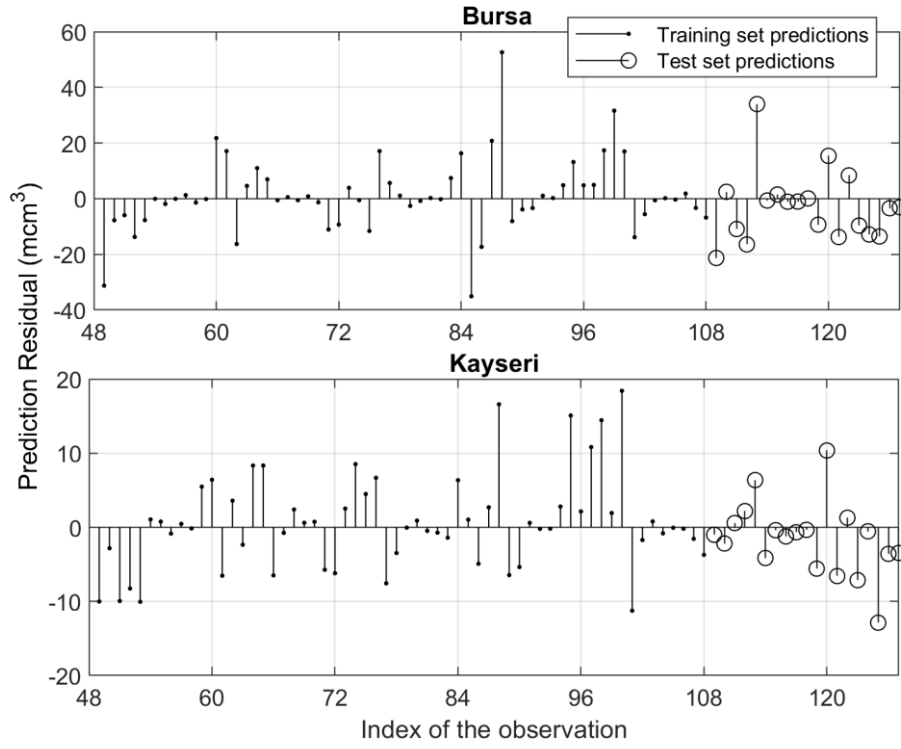


Figure 11. One-step ahead training set and multi-step ahead test set prediction residuals.

CONCLUSION AND RECOMMENDATIONS

NG is a pivotal source of energy, exhibiting a nearly constant yearly increase in worldwide demand over the past ~30 years. The reliance of numerous countries, including Turkey, on imports to maintain a sufficient NG supply underscores the significance of accurate NGDP in economic planning by governments. The present study examined the monthly NGDPs of two Turkish cities employing various time series models and a novel online learning method, JITL-GPR. Moreover, the JITL-GPR model demonstrated remarkable precision in forecasting the yearly NGD for 2023, achieving an out-of-sample prediction error of less than 1% for both Bursa and Kayseri.

The current methodology, in contrast to the utilization of each previous NGD value as a separate feature, i.e., in a separate column of a regressor matrix, employs a weighting system that considers the proximity of previous NGD values to the query point in months and years. This methodology then adjusts the weights to achieve the best fitting (in Bayesian sense) via GPR (see Equation 18). The present approach bears resemblance to the “kriging” method employed in geostatistics, wherein Gaussian processes are used in low-dimensional spatial dimensional settings [102]. The proposed method can be regarded as a regularized version of the standard prediction methods, wherein the input features are derived from lagged output values. In contrast to the SARIMAX method, which seeks to maximize the likelihood under the constraints of stability and invertibility, the proposed method employs a regularization approach that restricts the impact of NGD values from previous years and months on the current year, thereby ensuring proximity in year and month (weighted) directions. While this regularization may have led to an increase in bias in predictions, particularly under a batch learning strategy, the application of a nonlinear learner, such as GPR, is likely to maintain bias at a reasonable level, while effectively combating variance, and adapting to changing conditions. Resistance to outliers appears to be another advantage of JITL-GPR, attributable to the smoothing-out effect of the low-order kernel.

Despite the geographical separation of Bursa and Kayseri, which is approximately 660 km apart, both exhibit a Mediterranean and continental climate. However, comparable optimal window parameters for GPR-JITL were obtained in both locations. This congruence may be due to two potential factors: (i) an artifact resulting from the approximation used in aggregating months from January to May into a single category to address the issue of inadequate sample size, or (ii) medium-term (monthly) NGD values exhibiting reduced sensitivity to weather conditions, compared to social variables affecting a broader community or nation. This

observation, in conjunction with the selection of window parameters during winter months, requires further investigation. The automated procedure of lumping “similar” months is recommended to avoid selection bias. Additionally, the autocorrelation structure of the prediction residuals of GPR-JITL suggests that the proposed method may require further refinement to adapt to the rapid fluctuations in NGD, such as abrupt drifts. This may necessitate the incorporation of recent observations using, for instance, weighted GPR [103] or the integration of predictions with time series models within a transfer learning framework [66]. Finally, the incorporation of “Ramadan effect” [104] into the JITL-GPR framework, if it exists, could potentially enhance the accuracy of NGDP values. Further research is necessary to investigate these aspects and improve the prediction accuracy of NGD values.

REFERENCES

1. Taşpınar F, Çelebi N, Tutkun N. Forecasting of daily natural gas consumption on regional basis in Turkey using various computational methods. *Energy Build.* 2013;56: 23–31. doi:10.1016/j.enbuild.2012.10.023
2. Liu J, Wang S, Wei N, Chen X, Xie H, Wang J. Natural gas consumption forecasting: A discussion on forecasting history and future challenges. *J Nat Gas Sci Eng.* 2021;90: 103930. doi:10.1016/j.jngse.2021.103930
3. Meira E, Cyrino Oliveira FL, de Menezes LM. Forecasting natural gas consumption using Bagging and modified regularization techniques. *Energy Econ.* 2022;106: 105760. doi:10.1016/j.eneco.2021.105760
4. Li N, Wang J, Liu R, Zhong Y. What is the short-term outlook for the EU's natural gas demand? Individual differences and general trends based on monthly forecasts. *Environ Sci Pollut Res.* 2022;29: 78069–78091. doi:10.1007/s11356-022-21285-9
5. Sánchez-Úbeda EFco, Berzosa A. Modeling and forecasting industrial end-use natural gas consumption. *Energy Econ.* 2007;29: 710–742. doi:10.1016/j.eneco.2007.01.015
6. Berrisford HG. *The Relation between Gas Demand and Temperature: A Study in Statistical Demand Forecasting.* OR. 1965;16: 229–246. doi:10.2307/3007504
7. Durrer EJ, Somerton WH, Mueller TD. *Short-Range Multivariate Process Prediction for Use in Automatized Systems.* Available: <https://dx.doi.org/10.2118/2630-MS>
8. Box GEP, Jenkins GM. *Time Series Analysis: Forecasting and Control.* Holden-Day; 1970.
9. Herbert JH. Data analysis of sales of natural gas to households in the United States. *J Appl Stat.* 1986;13: 199–211. doi:10.1080/02664768600000028
10. Liu L-M, Lin M-W. Forecasting residential consumption of natural gas using monthly and quarterly time series. *Int J Forecast.* 1991;7: 3–16. doi:10.1016/0169-2070(91)90028-T
11. Suykens J, Lemmerling Ph, Favoreel W, de Moor B, Crepel M, Briol P. Modelling the Belgian gas consumption using neural networks. *Neural Process Lett.* 1996;4: 157–166. doi:10.1007/BF00426024
12. Khotanzad A, Elragal HM. Natural gas load forecasting with combination of adaptive neural networks. *IEEE;* 1999. doi:10.1109/IJCNN.1999.830812
13. Viet NH, Mandziuk J. Neural and fuzzy neural networks in prediction of natural gas consumption. *Neural Parallel Sci Comput.* 2005;265–286.
14. Liu H, Liu D, Zheng G, Liang Y, Ni Y. Research on natural gas load forecasting based on support vector regression. *Fifth World Congress on Intelligent Control and Automation (IEEE Cat No04EX788).* 2004. pp. 3591A – 3595. doi:10.1109/WCICA.2004.1343263
15. Gil S, Deferrari J. Generalized Model of Prediction of Natural Gas Consumption. *J Energy Resour Technol.* 2004;126: 90–98. doi:10.1115/1.1739239
16. Potočnik P, Soldo B, Šimunović G, Šarić T, Jeromen A, Govekar E. Comparison of static and adaptive models for short-term residential natural gas forecasting in Croatia. *Appl Energy.* 2014;129: 94–103. doi:10.1016/j.apenergy.2014.04.102
17. Zhu L, Li MS, Wu QH, Jiang L. Short-term natural gas demand prediction based on support vector regression with false neighbours filtered. *Energy.* 2015;80: 428–436. doi:10.1016/j.energy.2014.11.083
18. Sharma V, Cali Ü, Sardana B, Kuzlu M, Banga D, Pipattanasomporn M. Data-driven short-term natural gas demand forecasting with machine learning techniques. *J Pet Sci Eng.* 2021;206: 108979. doi:10.1016/j.petrol.2021.108979
19. Khani H, Farag HEZ. An Online-Calibrated Time Series Based Model for Day-Ahead Natural Gas Demand Forecasting. *IEEE Trans Ind Inform.* 2019;15: 2112–2123. doi:10.1109/TII.2018.2861390

20. Hribar R, Potočnik P, Šilc J, Papa G. A comparison of models for forecasting the residential natural gas demand of an urban area. *Energy*. 2019;167: 511–522. doi:10.1016/j.energy.2018.10.175
21. Du J, Zheng J, Liang Y, Lu X, Klemeš JJ, Varbanov PS, et al. A hybrid deep learning framework for predicting daily natural gas consumption. *Energy*. 2022;257: 124689. doi:10.1016/j.energy.2022.124689
22. Bai S, Huang X, Luo M, Su J. Deep hybrid models for daily natural gas consumption forecasting and complexity measuring. *Energy Sci Eng*. 2023;11: 654–674. doi:10.1002/ese3.1352
23. Iranmanesh H, Abdollahzade M, Miranian A. Mid-Term Energy Demand Forecasting by Hybrid Neuro-Fuzzy Models. *Energies*. 2012;5: 1–21. doi:10.3390/en5010001
24. Izadyar N, Ong HC, Shamshirband S, Ghadamian H, Tong CW. Intelligent forecasting of residential heating demand for the District Heating System based on the monthly overall natural gas consumption. *Energy Build*. 2015;104: 208–214. doi:10.1016/j.enbuild.2015.07.006
25. Safiyari MH, Shavvalpour S, Tarighi S. From traditional to modern methods: Comparing and introducing the most powerful model for forecasting the residential natural gas demand. *Energy Rep*. 2022;8: 14699–14715. doi:10.1016/j.egyr.2022.10.397
26. Sector Report, Republic of Turkiye Energy Market Regulatory Authority. [cited 19 Feb 2025]. Available: <https://www.epdk.gov.tr/Detay/Icerik/3-0-94/dogal-gazyillik-sektor-raporu>
27. Berk I, Ediger VŞ. A historical assessment of Turkey’s natural gas import vulnerability. *Energy*. 2018;145: 540–547. doi:10.1016/j.energy.2018.01.022
28. Soldo B. Forecasting natural gas consumption. *Appl Energy*. 2012;92: 26–37. doi:10.1016/j.apenergy.2011.11.003
29. AKPINAR M, YUMUŞAK N. Naive forecasting of household natural gas consumption with sliding window approach. *Turk J Electr Eng Comput Sci*. 2017;25: 30–45. doi:10.3906/elk-1404-378
30. Özmen A, Yılmaz Y, Weber G-W. Natural gas consumption forecast with MARS and CMARS models for residential users. *Energy Econ*. 2018;70: 357–381. doi:10.1016/j.eneco.2018.01.022
31. Özmen A. Sparse regression modeling for short- and long-term natural gas demand prediction. *Ann Oper Res*. 2023;322: 921–946. doi:10.1007/s10479-021-04089-x
32. Ozmen A. Multi-objective regression modeling for natural gas prediction with ridge regression and CMARS. *Int J Optim Control Theor Appl IJOCTA*. 2022;12: 56–65. doi:10.11121/ijocta.2022.1084
33. Yukseltan E, Yucekaya A, Bilge AH, Agca Aktunc E. Forecasting models for daily natural gas consumption considering periodic variations and demand segregation. *Socioecon Plann Sci*. 2021;74: 100937. doi:10.1016/j.seps.2020.100937
34. Yucesan M, Pekel E, Celik E, Gul M, Serin F. Forecasting daily natural gas consumption with regression, time series and machine learning based methods. *Energy Sources Part Recovery Util Environ Eff*. 2025;47: 4605–4620. doi:10.1080/15567036.2021.1875082
35. Balıkçı V, Gemici Z, Taner T, Dalkılıç AS. Forecasting natural gas demand in Istanbul by artificial neural networks method and planning of city gate stations. 2024 [cited 19 Feb 2025]. doi:10.17341/gazimmfd.1165734
36. ARAS H, ARAS N. Forecasting Residential Natural Gas Demand. *Energy Sources*. 2004;26: 463–472. doi:10.1080/00908310490429740
37. Kizilaslan R, Karlik B. Combination of neural networks forecasters for monthly natural gas consumption prediction. *Neural Netw World*. 2009;19: 191–199.

38. Bilici Z, Özdemir D, Temurtaş H. Comparative analysis of metaheuristic algorithms for natural gas demand forecasting based on meteorological indicators. *J Eng Res.* 2023;11: 259–265. doi:10.1016/j.jer.2023.100127
39. Sarak H, Satman A. The degree-day method to estimate the residential heating natural gas consumption in Turkey: a case study. *Energy.* 2003;28: 929–939. doi:10.1016/S0360-5442(03)00035-5
40. GORUCU FB. Evaluation and Forecasting of Gas Consumption by Statistical Analysis. *Energy Sources.* 2004;26: 267–276. doi:10.1080/00908310490256617
41. Karadede Y, Ozdemir G, Aydemir E. Breeder hybrid algorithm approach for natural gas demand forecasting model. *Energy.* 2017;141: 1269–1284. doi:10.1016/j.energy.2017.09.130
42. Toksari M. Predicting the Natural Gas Demand Based on Economic Indicators: Case of Turkey. *Energy Sources Part Recovery Util Environ Eff.* 2010;32: 559–566. doi:10.1080/15567030802578823
43. Ozdemir G, Aydemir E, Olgun MO, Mulbay Z. Forecasting of Turkey natural gas demand using a hybrid algorithm. *Energy Sources Part B Econ Plan Policy.* 2016;11: 295–302. doi:10.1080/15567249.2011.611580
44. Arık OA. Artificial bee colony algorithm to forecast natural gas consumption of Turkey. *SN Appl Sci.* 2019;1: 1138. doi:10.1007/s42452-019-1195-8
45. ES HA, Baban P, Hamzacebi C. Prediction of natural gas demand by considering implications of energy-related policies: The case of Türkiye. *Energy Sources Part B Econ Plan Policy.* 2023;18: 2274865. doi:10.1080/15567249.2023.2274865
46. Erdogdu E. Natural gas demand in Turkey. *Appl Energy.* 2010;87: 211–219. doi:10.1016/j.apenergy.2009.07.006
47. Melikoglu M. Vision 2023: Forecasting Turkey’s natural gas demand between 2013 and 2030. *Renew Sustain Energy Rev.* 2013;22: 393–400. doi:10.1016/j.rser.2013.01.048
48. Özcan T, Konyalıoğlu AK, Apaydın T. Forecasting natural gas consumption in Turkey using fractional non-linear grey Bernoulli model optimized by grey wolf optimization (GWO) algorithm. *Euro-Mediterr J Environ Integr.* 2024;9: 2039–2055. doi:10.1007/s41207-024-00618-9
49. Mittakola RT, Ciais P, Zhou C. Short-to-medium range forecast of natural gas use in the United States residential buildings. *J Clean Prod.* 2024;437: 140687. doi:10.1016/j.jclepro.2024.140687
50. Khan MA. Modelling and forecasting the demand for natural gas in Pakistan. *Renew Sustain Energy Rev.* 2015;49: 1145–1159. doi:10.1016/j.rser.2015.04.154
51. Göncü A, Karahan MO, Kuzubaş TU. Forecasting daily residential natural gas consumption: A dynamic temperature modelling approach. *Bogazici J.* 2019;33. doi:10.21773/boun.33.1.3
52. Vondráček J, Pelikán E, Konár O, Čermáková J, Eben K, Malý M, et al. A statistical model for the estimation of natural gas consumption. *Appl Energy.* 2008;85: 362–370. doi:10.1016/j.apenergy.2007.07.004
53. Kaynar O, Yilmaz I, Demirkoparan F. Forecasting of natural gas consumption with neural network and neuro fuzzy system. 2011 [cited 19 Feb 2025]. Available: <https://hdl.handle.net/20.500.12418/9677>
54. Beyca OF, Ervural BC, Tatoglu E, Ozuyar PG, Zaim S. Using machine learning tools for forecasting natural gas consumption in the province of Istanbul. *Energy Econ.* 2019;80: 937–949. doi:10.1016/j.eneco.2019.03.006
55. Es HA. Monthly natural gas demand forecasting by adjusted seasonal grey forecasting model. *Energy Sources Part Recovery Util Environ Eff.* 2021;43: 54–69. doi:10.1080/15567036.2020.1831656

56. Akpinar M, Yumusak N. Year Ahead Demand Forecast of City Natural Gas Using Seasonal Time Series Methods. *Energies*. 2016;9: 727. doi:10.3390/en9090727
57. Ceylan Z. Comparative analysis of deep learning and classical time series methods to forecast natural gas demand during COVID-19 pandemic. *Energy Sources Part B Econ Plan Policy*. 2023;18: 2241455. doi:10.1080/15567249.2023.2241455
58. Xu G, Chen Y, Yang M, Li S, Marma KJS. An outlook analysis on China's natural gas consumption forecast by 2035: Applying a seasonal forecasting method. *Energy*. 2023;284: 128602. doi:10.1016/j.energy.2023.128602
59. Zhang L, Ma X, Zhang H, Zhang G, Zhang P. Multi-Step Ahead Natural Gas Consumption Forecasting Based on a Hybrid Model: Case Studies in The Netherlands and the United Kingdom. *Energies*. 2022;15: 7437. doi:10.3390/en15197437
60. Gama J. A survey on learning from data streams: current and future trends. *Prog Artif Intell*. 2012;1: 45–55. doi:10.1007/s13748-011-0002-6
61. Ditzler G, Roveri M, Alippi C, Polikar R. Learning in Nonstationary Environments: A Survey. *IEEE Comput Intell Mag*. 2015;10: 12–25. doi:10.1109/MCI.2015.2471196
62. Hinder F, Vaquet V, Hammer B. One or two things we know about concept drift—a survey on monitoring in evolving environments. Part A: detecting concept drift. *Front Artif Intell Sec Mach Learn Artif Intell*. 2024;7. doi:10.3389/frai.2024.1330257.
63. Urhan A, Alakent B. Integrating adaptive moving window and just-in-time learning paradigms for soft-sensor design. *Neurocomputing*. 2020;392: 23–37. doi:10.1016/j.neucom.2020.01.083
64. Bontempi G, Ben Taieb S, Le Borgne Y-A. Machine Learning Strategies for Time Series Forecasting. In: Aufaure M-A, Zimányi E, editors. *Business Intelligence: Second European Summer School, eBISS 2012, Brussels, Belgium, July 15-21, 2012, Tutorial Lectures*. Berlin, Heidelberg: Springer; 2013. pp. 62–77. doi:10.1007/978-3-642-36318-4_3
65. Alakent B. Soft sensor design using transductive moving window learner. *Comput Chem Eng*. 2020;140: 106941. doi:10.1016/j.compchemeng.2020.106941
66. Alakent B. Soft-sensor design via task transferred just-in-time-learning coupled transductive moving window learner. *J Process Control*. 2021;101: 52–67. doi:10.1016/j.jprocont.2021.03.006
67. Makridakis S, Wheelwright SC, Hyndman RJ. *Forecasting methods and applications*. New York, US: Wiley; 1998.
68. Cleveland RB, Cleveland WS, McRae JE, Terpenning I. STL: A seasonal-trend decomposition procedure based on loess. *J Off Stat*. 1990;6: 3–73. Available: <http://www.nniem.ru/file/news/2016/stl-statistical-model.pdf>
69. Hyndman RJ, Athanasopoulos G. *Forecasting: principles and practice*. 3rd ed. Melbourne, Australia: OTexts; 2021. Available: https://www.academia.edu/download/64659947/Athanasopoulos__George__Hyndman__Rob_J._-_Forecasting__Principles_and_Practice_2018.pdf
70. Theodosiou M. Forecasting monthly and quarterly time series using STL decomposition. *Int J Forecast*. 2011;27: 1178–1195. doi:10.1016/j.ijforecast.2010.11.002
71. Hyndman RJ, Athanasopoulos G. *Forecasting: principles and practice*. 2nd ed. Melbourne, Australia: OTexts; 2018. Available: https://www.academia.edu/download/64659947/Athanasopoulos__George__Hyndman__Rob_J._-_Forecasting__Principles_and_Practice_2018.pdf
72. Box GE, Jenkins GM, Reinsel GC. *Time series analysis: forecasting and control*. Englewood Cliffs, NJ: Prentice Hall; 1994.
73. Hyndman R, Koehler AB, Ord JK, Snyder RD. *Forecasting with exponential smoothing: the state space approach*. Berlin: Springer-Verlag; 2008.

74. Aoki M. State space modeling of time series. 2nd ed. Berlin: Springer-Verlag; 1990.
75. Brown RG. Statistical forecasting for inventory control. McGraw-Hill; 1959.
76. Holt CC. Forecasting seasonals and trends by exponentially weighted moving averages. *Int J Forecast*. 2004;20: 5–10. doi:10.1016/j.ijforecast.2003.09.015
77. Winters PR. Forecasting Sales by Exponentially Weighted Moving Averages. *Manag Sci*. 1960;6: 324–342. doi:10.1287/mnsc.6.3.324
78. Gardner ES. Exponential smoothing: The state of the art. *J Forecast*. 1985;4: 1–28. doi:10.1002/for.3980040103
79. De Livera AM, Hyndman RJ, Snyder RD. Forecasting Time Series With Complex Seasonal Patterns Using Exponential Smoothing. *J Am Stat Assoc*. 2011;106: 1513–1527. doi:10.1198/jasa.2011.tm09771
80. Isikli E, Temizer L, Kazdaloglu AE, Ari E. Time Series Analysis. In: Ustundag A, Cevikcan E, Beyca OF, editors. *Business Analytics for Professionals*. Cham: Springer International Publishing; 2022. pp. 113–125. doi:10.1007/978-3-030-93823-9_4
81. Yang Y. Combining forecasting procedures: some theoretical results. *Econom Theory*. 2004;20: 176–222. doi:10.1017/S0266466604201086
82. Qian W, Rolling CA, Cheng G, Yang Y. Combining forecasts for universally optimal performance. *Int J Forecast*. 2022;38: 193–208. doi:10.1016/j.ijforecast.2021.05.004
83. Borthakur P, Goswami B. Short term load forecasting: A hybrid approach using data mining methods. Patna, India: IEEE; 2020. pp. 1–6. doi:10.1109/ICEFEET49149.2020.9187009
84. Zou H, Yang Y. Combining time series models for forecasting. *Int J Forecast*. 2004;20: 69–84. doi:10.1016/S0169-2070(03)00004-9
85. Wei X, Yang Y. Robust forecast combinations. *J Econom*. 2012;166: 224–236. Available: <https://www.sciencedirect.com/science/article/pii/S0304407611002168>
86. Bishop CM. *Pattern recognition and machine learning*. New York Springer; 2006.
87. Rasmussen CE, Williams CKI. *Gaussian Processes for Machine Learning*. Available: <https://direct.mit.edu/books/monograph/2320/Gaussian-Processes-for-Machine-Learning>
88. Cleveland WS. Robust Locally Weighted Regression and Smoothing Scatterplots. *J Am Stat Assoc*. 1979;74: 829–836. doi:10.1080/01621459.1979.10481038
89. Aha DW, Kibler D, Albert MK. Instance-based learning algorithms. *Mach Learn*. 1991;6: 37–66. doi:10.1007/BF00153759
90. Kibler D, Aha DW, Albert MK. Instance-based prediction of real-valued attributes. *Comput Intell*. 1989;5: 51–57. doi:10.1111/j.1467-8640.1989.tb00315.x
91. Bontempi G, Birattari M, Bersini H. Lazy learning for local modelling and control design. *Int J Control*. 1999;72: 643–658. doi:10.1080/002071799220830
92. Öberg T, Liu T. Global and Local PLS Regression Models to Predict Vapor Pressure. *QSAR Comb Sci*. 2008;27: 273–279. doi:10.1002/qsar.200730038
93. Macciò D, Cervellera C. Local Models for data-driven learning of control policies for complex systems. *Expert Syst Appl*. 2012;39: 13399–13408. doi:10.1016/j.eswa.2012.05.063
94. Cheng C, Chiu M-S. A new data-based methodology for nonlinear process modeling. *Chem Eng Sci*. 2004;59: 2801–2810. doi:10.1016/j.ces.2004.04.020
95. Fujiwara K, Kano M, Hasebe S, Takinami A. Soft-sensor development using correlation-based just-in-time modeling. *AIChE J*. 2009;55: 1754–1765. doi:10.1002/aic.11791
96. Alakent B. Online tuning of predictor weights for relevant data selection in just-in-time-learning. *Chemom Intell Lab Syst*. 2020;203: 104043. doi:10.1016/j.chemolab.2020.104043
97. Karunasingha DSK. Root mean square error or mean absolute error? Use their ratio as well. *Inf Sci*. 2022;585: 609–629. doi:10.1016/j.ins.2021.11.036

98. Shcherbakov MV, Brebels A, Shcherbakova NL, Tyukov AP, Janovsky TA, Kamaev VA. A survey of forecast error measures. *World Appl Sci J.* 2013;24: 171–176. doi:10.5829/idosi.wasj.2013.24.itmies.80032
99. Isikli E, Serdarasan S. The Power of Combination Models in Energy Demand Forecasting. In: Kayakutlu G, Kayalica MÖ, editors. *Decision Making Using AI in Energy and Sustainability.* Cham: Springer International Publishing; 2023. pp. 153–167. doi:10.1007/978-3-031-38387-8_9
100. Wright MH. The interior-point revolution in optimization: History, recent developments, and lasting consequences. *Bull Am Math Soc.* 2005;42: 39–56. doi:10.1090/S0273-0979-04-01040-7
101. Gawel B, Paliński A. Global and Local Approaches for Forecasting of Long-Term Natural Gas Consumption in Poland Based on Hierarchical Short Time Series. *Energies.* 2024;17: 347. doi:10.3390/en17020347
102. Spatial Prediction and Kriging. *Statistics for Spatial Data.* John Wiley & Sons, Ltd; 1993. pp. 105–209. doi:10.1002/9781119115151.ch3
103. Sheng H, Liu X, Bai L, Dong H, Cheng Y. Small sample state of health estimation based on weighted Gaussian process regression. *J Energy Storage.* 2021;41: 102816. doi:10.1016/j.est.2021.102816
104. Sonjaya AR, Wahyudi I. The Ramadan effect: Illusion or reality? *Arab Econ Bus J.* 2016;11: 55–71. doi:10.1016/j.aebj.2016.03.001
105. Akpınar M, Adak MF, Yumusak N. Day-ahead natural gas demand forecasting using optimized ABC-based neural network with sliding window technique: The case study of regional basis in Turkey. *Energies.* 2017;10: 781. doi:10.3390/en10060781

Appendix:

Summary of NGDM Studies in Turkey

Reference	City *	Prediction (Forecast) Horizon **	Data Frequency	Database	Train/Test/Validation Ratio	Methods Used	Best Method	Performance Indicators Used	Temperature	Humidity	Wind	Public Holidays	Calendar Data (Weekday/Weekend)
[35]	I	D, H	2008-2018 daily consumption	Istanbul Gas Distribution Company (IGDAS)	75-15-10	ANN	-	MSE	√	X	X	√	X
[48]	-	A	2004-2012 annual consumption	Republic of Turkey Energy Market Regulatory Authority	75-25-0	GWO-FANGBM, GWO-GM, GM, ARIMA, LR	GWO-FANGBM	MAE, MAPE, RMSE	X	X	X	X	X
[57]	-	W	March 2020-March 2022	Turkish Ministry of Energy and Natural Resources	70-30-0	ARIMA, NARNN, SVR, LSTM	LSTM	RMSE, MAE	X	X	X	X	X
[31]	AN	A, D, W	2004-2013 daily consumption	Başkentgaz	60-40-0	LR, MARS, LASSO	MARS	MAPE, maxAPE, AAE, RMSE, R^2	√	√	√	X	√
[45]	-	A	2000 to 2019 annual consumption	BP Report (https://www.bp.com/)	80-20-0	Grey Prediction Models, GM Verhulst, Dynamic Grey Models	GM(1,5)	MAPE, RMSE, MSPE	X	X	X	X	X
[38]	-	M	2010-2020 monthly consumption	jodidata.org	73-27-0	DEA, PSO, GSA and BSO Linear and Quadratic Models	PSO-Q	MAE, MAPE, RMS, MARNE, R^2	√	√	√	X	X
[32]	AN	D, W	2004-2013 daily consumption	Başkentgaz	60-40-0	Ridge Regression, CMARS	CMARS	MAPE, AAE, RMSE, R^2	√	√	√	X	X

Reference	City *	Prediction (Forecast) Horizon **	Data Frequency	Database	Train/Test/Validation Ratio	Methods Used	Best Method	Performance Indicators Used	Temperature	Humidity	Wind	Public Holidays	Calendar Data (Weekday/Weekend)
[33]	AN, B, E, I	A, D, M, W	2002–2017 daily consumption	BOTAS Petroleum Pipeline Corporation	-	Fourier Series Expansion (FSE), Fourier Series Expansion with Temperature (FSET), Fourier Series Expansion with Temperature and Feedback (FSETF), AR Models	Fourier Series Expansion with Temperature and Feedback (FSETF)	MAPE, RMSE	√	X	X	X	X
[34]	-	D	2017–2019 daily consumption	Ministry of Energy and Natural Resources	70-30-0	ARIMAX, SARIMAX, ANN, NARX, LSTM, ARIMAX-ANN, SARIMAX-ANN, GA-ANN, PSO-ANN	SARIMAX-ANN	MAPE, RMSE, MSE, R^2	X	X	X	X	√
[55]	-	M	2000–2018 monthly consumption	International Energy Agency	75-25-0	Seasonal Grey Forecasting Model, Adjusted Seasonal Grey Forecasting Model, SARIMA	Adjusted Seasonal Grey Forecasting Model	MAPE, MAE, RMSE, post-error ratio	X	X	X	X	X
[44]	-	A	1998–2017 annual consumption	EnerData https://www.enerd.ata.net/	-	Artificial Bee Colony (ABC) Algorithm, Multiple Linear Regression	Artificial Bee Colony (ABC) Algorithm	MAPE	X	X	X	X	X
[54]	I	M	2005–2015 monthly consumption	Istanbul Gas Distribution Company (IGDAS)	90-10-0	Multiple Linear Regression, ANN, SVM	SVM	MAPE, R^2	√	X	X	X	X
[30]	AN	D	2009–2013 daily consumption	Başkentgaz	80-20-0	Linear Regression, NN, MARS, CMARS	CMARS	AAE, RMSE, MAPE	√	√	√	X	√

Reference	City *	Prediction (Forecast) Horizon **	Data Frequency	Database	Train/Test/Validation Ratio	Methods Used	Best Method	Performance Indicators Used	Temperature	Humidity	Wind	Public Holidays	Calendar Data (Weekday/Weekend)
[41]	-	A	1985-2000 annual consumption	Turkish Statistical Institute	-	Nonlinear Regression, Nonlinear Regression-based Breeder Genetic Algorithm, Nonlinear Regression-based Breeder Genetic Algorithm and Simulated Annealing	Nonlinear Regression-based Breeder Genetic Algorithm and Simulated Annealing	MAPE	X	X	X	X	X
[105]	A	D	2011-2014 households and low-consuming commercial users' daily consumption	Adapazarı Natural Gas Distribution Company (AGDAS)	75-25-0	Artificial Bee Colony-based Artificial Neural Networks (ANN-ABC), ANN-BP Algorithm	Artificial Bee Colony-based Artificial Neural Networks (ANN-ABC)	MAPE, MSE, R^2	X	X	X	X	X
[29]	A	D	2011-43 days 2012-366 days	Adapazarı Natural Gas Distribution Company (AGDAS)	-	Multiple Linear Regression	-	MAPE	√	√	X	√	√
[56]	A	M	2011-2014 monthly consumption	Adapazarı Natural Gas Distribution Company (AGDAS)	75-25-0	Holt-Winters Exponential Smoothing, ARIMA, SARIMA	ARIMA	MAPE, R^2 , AIC, BIC	X	X	X	X	X
[43]	-	A	1985-2010 annual consumption	Ministry of Energy and Natural Resources	65-35-0	Hybrid Genetic Algorithm-Simulated Annealing (GA-SA) Algorithm, Multiple Linear Regression	GA-SA	MAPE, RE	X	X	X	X	X
[1]	A	D	2007-2011 daily consumption	Adapazarı Natural Gas Distribution Company (AGDAS)	71-29-0	SARIMAX, ANN-MLP, ANN-RBF, Multivariate OLS	ANN-MLP	MAPE, RMSE	√	√	√	X	X

Reference	City *	Prediction (Forecast) Horizon **	Data Frequency	Database	Train/Test/Validation Ratio	Methods Used	Best Method	Performance Indicators Used	Temperature	Humidity	Wind	Public Holidays	Calendar Data (Weekday/Weekend)
[47]	-	A	1987-2011 annual consumption	BOTAS Petroleum Pipeline Corporation	-	Linear and Logistic Models	Linear Models	RMSE, MAPE, R^2	X	X	X	X	X
[51]	I	D	2004-2011 daily consumption	Istanbul Gas Distribution Company (IGDAS)	-	Analytical Model, Monte Carlo Simulation	-	RMSE	√	√	X	√	√
[53]	-	W	2002-2006 weekly consumption	BOTAS Petroleum Pipeline Corporation	80-20-0	ARIMA, ANN-MLP, ANN-RBF, ANNFIS	ANFIS	MAPE, RMSE	X	X	X	X	X
[42]	-	A	1984-2006 annual consumption	Ministry of Energy and Natural Resources	-	Linear and Quadratic Simulated Annealing	-	Absolute Value of Relative Errors	X	X	X	X	X
[37]	I	M	2004-2007 monthly consumption	Istanbul Gas Distribution Company (IGDAS)	60-20-20	ANN	-	ARE, R^2	√	X	X	X	X
[40]	AN	A	1991-2001	BOTAS Petroleum Pipeline Corporation	-	Multiple Linear Regression	-	R^2	√	X	X	X	X
[36]	I, AN, B, E, K	M	1996-2001 monthly consumption	EGO, IGDAS, BURSAGAZ, ESGAZ, IZGAZ	-	Autoregressive Time Series Models	-	MAPE, MAE, MSE, R^2	√	X	X	X	X

* A: Adapazarı, AN: Ankara, B: Bursa, E: Eskisehir, I: Istanbul, K: Kocaeli

** A: Annually, D: Daily, M: Monthly, Q: Quarterly, W: Weekly